

高振動励起分子の性質とダイナミックス の理論的研究

(課題番号01540396)

1990、1991年度科学研究費補助金 一般研究(C)
研究成果報告書

1991年3月

研究代表者 高塚 和夫

(名古屋大学教養部助教授)

KAKEN
01540396
集

1990、1991年度科学研究費補助金 一般研究(C)
研究成果報告書

(課題番号01540396)

高振動励起分子の性質とダイナミックスの
理論的研究

研究組織

研究代表者： 高塚 和夫 (名古屋大学教養部助教授)

研究経費

1989年度	1300千円
1990年度	300千円
計	1600千円

名古屋大学図書	
和B	69395

研究発表

(1) 学会誌等

a) K. Takatsuka

Density of States for Chaotic Systems in Phase-Space Semiclassical Mechanics.

J. Math. Phys. 投稿中

b) K. Takatsuka

Extraction of Accurate Frequencies from Fast-Fourier-Transform Spectra.

J. Compt. Phys. 投稿中

c) K. Takatsuka

Possible Onset of Entrainment in Hamiltonian Chaos.

Phys. Rev. A 投稿準備中

d) K. Takatsuka

Action and Quasi-Action Variables in Molecular Vibrations.

Phys. Rev. A 投稿準備中

(2) 口頭発表

a) 高塚和夫

波動関数の動力学的分解

化学反応討論会、1989年6月27日（大阪）

b) 高塚和夫

Phase-Space Path Integrals.

1989環太平洋国際化学会議、12月23日（ハワイ）

c)K. Takatsuka

Periodic Orbit Theory in Phase-Space Semiclassical Mechanics.

Workshop of Quantum Chaos, June 12 1990 (Trieste, Italy)

d) 高塚和夫

振動カオスの秩序構造 -作用変数と擬作用変数-

分子構造総合討論会、1990年10月15日(九州大学)

本研究の目的は、分子の高振動励起状態の性質とそのダイナミクス等に関する基礎的な運動法則を明かにすることである。高振動励起状態の分子運動を特徴付けるのは、所謂カオスと呼ばれる、見かけ上極めて複雑かつ乱雑な運動様式である。カオスは、現代科学の最も包括的な概念の一つであって、自然現象の至る所で観察することができる。化学現象に即して言うならば、それは、高振動励起状態のみならず、化学反応の遷移状態近傍や、単分子分解における分子内エネルギー移動、理論的に確認は未だされていないが、溶液やクラスターのダイナミクスなどで見ることができる。ただ、分子の場合には、本質的に量子力学の制約を受けるために、特に量子カオスと呼ばれる分野を成しているということになる。しかし、化学の場合には、レーザー技術の発展のため良質な分光学的データを得ることができ、今後さらに、量子カオスの中における重要性を増すであろう。

一方、分子がカオスの性格を持ちやすいということは、分子運動が古典力学的性質を強く持つということに拠っている。つまり、分子は、電子などに比べて、はるかに重いということである。このように、古典力学的性質を強く持つ量子系を扱う際には、半古典力学を適用せざるを得ない。この領域では、分子は非常に短い波長の物質波を持ち、従って極めて高い状態密度を持つことになる。更に、高い状態密度は必然的に系に統計力学的性質をもたらす。化学反応の速度過程がしばしば単純統計論で処理されるのは、このためである。

本課題研究では、上の観点に立って、比較的一般的な（量子）カオスの立場から、状態密度の決定や、カオスへの遷移の問題を取り扱った。本研究で現在までに明らかになったことは、概略、以下の通りである：

(1) 筆者が開発した位相空間経路積分の方法を分子振動の量子化の問題に適用し、状態密度の一般的表式を得た。（論文a）この際、系が可積分の場合には所謂 EBK 条件が得られ、非可積分（カオス）の場合には、Gutzwiller の式を拡張したものが得られた。更に、非可積分系は、二つの場合に分けられる。系が不安定な周期軌道を持つ場合には、状態密度はそれらの軌道のエネルギー位置でローレンツ型ピークを持ち、その高さは軌道の安定度に逆比例する。一方、安定な周期軌道を持つ場合には、共鳴型の量子条件を持つ事が統一的に示された。特に後者の場合、現に実験で得られている準カオス系のスペクトルの解釈に重大な示唆を与えるものとなっており、今後の発展が期待される。

(2)論文aでは更に、量子化という観点からカオスを弱いものと強いものに分け、それを判定する条件を検討した。

(3)量子化規則の中に現われるトポロジカルな量であるマスロフ指数の、位相空間における非常に単純な幾何学的意味づけを見いだした。また、古典カオスで常用される判定条件の一つであるリアプノフ指数が量子力学から自然に導かれることを示した。また、大局的カオスの判定条件として有名なグリーンの留数がやはり、量子力学から自然に出てくる量であることも分かった。筆者の主張は、これら三つの量が全て、位相空間経路積分の半古典的表式の中の振幅項から統一的に導かれるということである。

(4)位相空間における周期軌道の理論に立脚して、エントロピーや温度の概念に検討を加えた。(論文a) 特に、作用積分の虚数部分が温度の逆数に対応していることを、この理論の枠組みの中で、主張した。これは、今後の本研究の重要な展開点になると思う。

(5)分子振動による運動が可積分か非可積分(局所的カオス)かを判定するには、つまり、系のカオスへの遷移を判定するには、直接、作用変数を計算すればよい。本研究では、分子の作用変数を実際的に計算する手法を位相空間の幾何学に基づいて開発した。これにより、相当大きな分子の振動量子化が行なえるようになった。(論文c、d)

(6)これに関連して、高速フーリエ変換のスペクトルから精度の高い周波数と振幅を計算するアルゴリズムを同時に開発した。(論文b) これは、高速フーリエ変換を使って離散スペクトルを同定しようとする全ての問題に応用できる。

(7)更に、作用変数の近似概念として擬作用変数というものを定義した。(論文c、d) 擬作用変数はカオス系では連続スペクトルを与えるが、これを調べることにより、位相空間内で異なる多様体が接合することによる連続スペクトルの発生や引込現象に類似のスペクトルの存在などを見いだした。また、この理論を使って一次共鳴の研究等が現在も進行中である。

DENSITY OF STATES FOR CHAOTIC SYSTEMS IN PHASE-SPACE SEMICLASSICAL MECHANICS

Kazuo Takatsuka
College of General Education
Nagoya University
Nagoya 464-01, Japan

The periodic orbit theory for calculating density of states in a chaotic Hamiltonian system is discussed within our framework of phase-space semiclassical mechanics. An extended expression of the density of states in chaos is derived, through which a possibility of assigning the "quantum numbers" and their roles for irregular spectra are discussed. It is also shown that a systematic application of the periodic orbit theory in phase space leads to the EBK quantum conditions for integrable systems, and also to a quantum condition for a stable but non-integrable system. A simple interpretation of the geometrical meaning of the so-called Maslov index in the quantum conditions is given. An attempt is made to analyze the Boltzmann entropy of microcanonical ensemble in terms of the dynamics relevant to quantum chaos.

I. INTRODUCTION

Since the first mathematical expression for the density of states of a classically chaotic system was given by Gutzwiller¹, the so-called periodic orbit theory^{1,2} has been argued extensively in the field of quantum chaos from various points of view such as the number of quantum numbers,^{3a} the treatment of the Maslov index,^{3b,3c} and the relationship of the periodic orbit theory to the Einstein-Brillouin-Keller (EBK) conditions⁴. After these close theoretical studies, also with numerical examinations,^{5,6,7} the essential validity of the periodic theory seems to be recognized well these days.⁸ Nonetheless, the trace formula involved in the theory is still stated to be "very difficult". Recently Littlejohn⁹ has established an elegant theory which gives a new way of looking at the Lagrangian manifolds in quantum theory, which can lead to the trace formula more naturally.

In this paper we would like to present another way of constructing the density of states both for regular and chaotic systems systematically in terms of a phase-space semiclassical mechanics,¹⁰ which we call the dynamical characteristic function (DCF) formalism.¹¹ Roughly speaking, setting up the quantum conditions is equivalent to measuring the size of phase space manifolds such as invariant tori and periodic orbits in units of the length of matter wave. This is a part of reasons why the trace formula considered in the configuration (q) space¹ is very difficult and also why the phase space approach can give more transparent view. Through our reconsideration of the periodic orbit theory, we will elucidate the following points:

(1) An extended expression of the density of states in chaos is given, Eq.(5-7) in Sec.V, in which the "quantum numbers" are found to be associated with each quantized periodic orbit. The possibility of experimental assignment of the quantum numbers to irregular spectra and their roles are discussed (Sec.VI). A modified version of the ergodic hypothesis relevant to quantum chaos is proposed, and a qualitative argument on the relationship between the

Boltzmann entropy in a microcanonical ensemble and quantum chaos is also presented (Sec.VI).

(2) The relationship between the density of states of a non-integrable system and that of an integrable one in resonance is clarified.

(3) The EBK conditions (conditions for multiply periodic orbits, which are topologically different from pure periodic orbits) are derived within the framework of the present periodic-orbit theory. In the integrable case, the quantum conditions for resonant and non-resonant cases are distinguished. (Sec.IV)

(4) A simple geometrical interpretation of the Maslov index is given in the context of the topological nature of a volume element which is to be carried by phase flow along a periodic orbit (Sec.III).

(5) It will be shown that some indices commonly recognized as being characteristic to classical chaos such as the Liapounov exponent¹² and Greene's residue¹³ are naturally derived from the amplitude factor of DCF (Sec.II). The KS-entropy¹² is also discussed in the context of quantum theory, and we define a new dynamical entropy which is relevant to the periodic orbit theory (Sec.VI).

The present paper begins with a brief review of the DCF theory in the next section.

II. SEMICLASSICAL MECHANICS

The theory starts with the definition of a phase space function¹¹

$$\begin{aligned} a(\phi_f \eta_f \xi_f : \phi_i \eta_i \xi_i) \\ = \int dq \phi_f(q + \eta_f) \phi_i^*(q + \eta_i) \exp[q(\xi_i - \xi_f)/\hbar], \end{aligned} \quad (2-1)$$

which is called DCF. Here ϕ_j and ϕ_f are mutually independent wave functions, and they can have even different time arguments. η and ξ (with suffices i and f) have dimensions of length and momentum, respectively, and thus DCF is a function defined in phase space.

Obviously, the variables η_j and η_f (and ξ_j and ξ_f) are not independent of each other in Eq.(2-1). Nonetheless, the arguments in Eq.(2-1) are put into the groups in that manner since the following property, the association rule, holds such that

$$(2\pi\hbar)^{-N} \int dZ_2 a(\phi_A Z_3 : \phi_B Z_2) a(\phi_B Z_2 : \phi_C Z_1) = a(\phi_A Z_3 : \phi_C Z_1), \quad (2-2)$$

where a short-handed notation of a phase space point is used, that is $Z_k = (\eta_k, \xi_k)$ ($k=1,2,3$). Here an arbitrary wave-packet state ϕ_B has been assumed to be normalized to unity. This association rule sets the foundation of a phase-space path-integral formalism. In order to go beyond the formalism of wave packet evolution, we define another DCF, the identity DCF, by

$$a_I(\eta_f \xi_f t_f : \eta_i \xi_i t_i) = \int dq K(q + \eta_f, q + \eta_i, t_f - t_i) \exp[q(\xi_i - \xi_f)/\hbar], \quad (2-3)$$

where K is the Feynman kernel, the explicit form of which is well-known in case where $t_f - t_i$ is infinitesimal. The successive applications of the association rule for the identity DCF

having an infinitesimal time-increment give a semiclassical form of the identity DCF with a finite time-interval. Instead of writing down it explicitly, we consider the following integral using the semiclassical DCF

$$\langle \Phi | e^{-iHt/\hbar} | \phi \rangle = (2\pi\hbar)^{-N} e^{-iN\pi/2} \int dZ_i a(\phi, Z_i; \Phi, Z_f) \times \left[\det \left\{ \frac{\partial(Z_f - Z_i)}{\partial Z_i} \right\} \right]^{1/2} \exp \left[\frac{i}{\hbar} S(Z_f, Z_i, t) \right], \quad (2-4)$$

where N is the physical dimension, Z_f is the end point of a classical trajectory starting from Z_i for time t , and S is the action integral taken along the path. In a phase space scheme, the branches of the action are automatically specified, and therefore S is characterized in terms of Z_i and Z_f . The first term in the integrand of Eq.(2-4) is a DCF representing the "initial condition" for each orbit. (Note the symmetric appearance of ϕ and Φ .) The second term is an amplitude factor which is to be described in a greater detail later. All the possible trajectories should be run and summed up, each having contributions from the amplitude, phase, and initial condition. The integral having the form of Eq.(2-4) appears in the S-matrix, time correlation of wave packets,^{14a} density of states, quantum scars,¹⁴ and so on, with ϕ and Φ chosen in appropriate forms.

The amplitude factor in Eq.(2-4) has many interesting properties in conjunction with classical chaos. Inside it we observe the following Jacobian *determinant* $\partial(Z_f - Z_i)/\partial Z_i$. Let $\exp(ib_k)$ and $\exp(-ib_k)$ ($k=1, \dots, N$) be the eigenvalues of the Jacobian *matrix* $[\partial Z_f/\partial Z_i]$. If some of b_k 's happen to be complex valued, the trajectory undergoes exponentially divergent separation from some of its neighboring trajectories which are set infinitesimally close at the outset. This is *local* chaos.¹² If, on the other hand, all the b_k 's are real, the trajectory is said to be stable. Let us first rewrite Eq.(2-4) in terms of b_k 's using the following identity

$$\partial(Z_f - Z_i)/\partial Z_i = \prod_{k=1}^N [(\exp(ib_k) - 1)(\exp(-ib_k) - 1)] = \prod_{k=1}^N \left[2 \sin\left(\frac{b_k}{2}\right) \right]^2. \quad (2-5)$$

Thus we have

$$\langle \Phi | e^{-iHt/\hbar} | \phi \rangle = (2\pi\hbar)^{-N} \int dZ_i a(\phi Z_i; \Phi Z_f) \prod_{k=1}^N \left[\frac{2}{i} \sin\left(\frac{b_k}{2}\right) \right] \exp\left[\frac{i}{\hbar} (S(Z_f, Z_i, t))\right]. \quad (2-6)$$

This is the basic equation for our analysis of the density of states.

Suppose that we observe classical chaos through the imaginary part of b_k 's, and let L be the sum of them which are positive and larger than a certain critical value. Then we can express as (see Eq.(2-5))

$$\prod_{k=1}^N \left[\frac{2}{i} \sin\left(\frac{b_k}{2}\right) \right] = \exp\left(\frac{L}{2}\right) \prod_{k=1}^{\prime} \left[\frac{2}{i} \sin\left(\frac{b_k}{2}\right) \right], \quad (2-7)$$

where the product in the right hand side is composed of b_k 's which are not used in L . The argument L is called the Liapounov exponent in the study of classical chaos. (Note that some slight difference in the definition can be present depending on the method of practical calculation.¹²⁾ It is intriguing that the Liapounov exponent is derived from quantum mechanics.

It is trivial to see the following identity hold for a general 2 by 2 matrix,

$$\det(M - I) = 2 - \text{Tr}(M). \quad (2-8)$$

If M is the tangent map of the Poincaré surface of section for a periodic orbit, then $2\text{-Tr}(M)$ is identical with $4R$, where R is the residue of Greene.¹³ R is known to be an extremely important quantity to judge the *global* occurrence of classical chaos.¹² We have already considered the left hand side of Eq.(2-8), if M is identified as the Jacobian matrix $[\partial Z_f/\partial Z_i]$. Since the matrix $[\partial(Z_f - Z_i)/\partial Z_i]$ in Eq.(2-5) is not restricted to be 2 by 2, its determinant can be regarded as a natural generalization of Greene's residue. (Note, however, that unlike Greene's M , $[\partial Z_f/\partial Z_i]$ includes the information about not only transversal directions to the periodic orbit but the parallel one.¹³)

Before closing this section we should comment on the convention of choosing the branches of the square root of Eq.(2-4) [cf. Eq.(2-5)]. Due to the real valuedness and symplectic property of $[\partial Z_f/\partial Z_i]$, ib always appear as a quadruplet set $\{ib, -ib, ib^*, -ib^*\}$, provided that they are complex. (The suffices are ignored for a moment.) Noting that $\exp(ib)$'s, not b 's themselves, are to be obtained as the eigenvalues of $[\partial Z_f/\partial Z_i]$, we consider a complex plane B on which the roots $\{ib, -ib, ib^*, -ib^*\}$ sit. Define

$$ib = c + id \quad (b = d - ic). \quad (2-9)$$

In case of nonzero c , we have to take ib and $-ib^*$ from $\{ib, -ib, ib^*, -ib^*\}$ to apply Eq.(2-5), and concomitantly the following product

$$\left[\frac{2}{i} \sin\left(\frac{b}{2}\right) \right] \left[\frac{2}{i} \sin\left(\frac{-b^*}{2}\right) \right] \quad (2-10)$$

appears in the magnitude part of Eq.(2-6). In what follows, Eq.(2-6) is understood in this form implicitly. We take a convention that the roots are selected from the right-half of the B -plane. Thus for an imaginary case, we pick up a pair of roots

$$ib = c + id \quad \text{and} \quad -ib^* = c - id \quad (c \geq 0). \quad (2-11)$$

On the other hand, in cases of elliptic ($ib = \pm id$), hyperbolic ($ib = \pm c$), and hyperbolic with-reflection^{6a} ($ib = \pm c - i\pi$ or $ib = \pm c + i\pi$) fixed points, we do not have a quadruple but a pair of roots on the B-plane. In elliptic case, ib to be used in Eq.(2-6) is picked up from the positive (negative) imaginary axis for $t > 0$ ($t < 0$). For a hyperbolic case, the root is taken from the positive real axis for all time, and in the case of hyperbolic-with-reflection, the root are selected from the upper right-half plane for the positive time and the lower right-half plane in the negative time. These are summarized are Table I. With this convention, the time reversal symmetry of DCF is conserved,¹¹ and also it is always connected smoothly as a function of time. Since there is no part of taking an absolute value in the amplitude factor in the value of Eq.(2-6), we should have no additional phase factor in DCF. This should be compared with the Maslov and Morse indices to be considered as a sudden jump of quantum phase for the semiclassical Feynman kernel and the WKB wave functions at caustics.¹⁵

III. DENSITY OF STATES IN TERMS OF DCF

A. Density of States

After the general manner due to Gutzwiller,¹ we try to write down the density of states as follows,

$$D(E) = \text{Tr} \delta(E - H) = \sum_i \delta(E - E_i) = (2\pi\hbar)^{-1} \int_{-\infty}^{\infty} dt \int dq \langle q | e^{-iHt/\hbar} | q \rangle e^{iEt/\hbar}. \quad (3-1)$$

The kernel part in this integrand can be replaced by Eq.(2-6) with adopting $\phi=q$ and $\Phi=q$. The DCF in Eq.(2-6) can now be integrated exactly over the q -coordinates as

$$\int_{-\infty}^{\infty} dq a(|q\rangle Z_i : |q\rangle Z_f) = (2\pi\hbar)^N \delta(Z_f - Z_i). \quad (3-2)$$

The δ function here directly indicates that the classical trajectories contributing to $D(E)$ must be perfectly periodic as originally discovered by Gutzwiller.¹ The present condition Eq.(3-2), which we call the strict periodic-orbit condition, is too strong, since the integration in it is performed in the range from $-\infty$ to ∞ . In reality, however, the information about bound states could be acquired in some much smaller finite region, which will reduce Eq.(3-2) to a less sharp function. This is a rather essential point in our approach and we will come back to this problem later. For the time being, the strict periodic-orbit condition is adopted. Then we have

$$D(E) = (\pi\hbar)^{-1} Re \int_0^{\infty} dt \int dZ_i \delta(Z_f - Z_i) \prod_{k=1}^N \left(\frac{2}{i} \sin\left(\frac{b_k}{2}\right) \right) \exp\left[\frac{i}{\hbar} (S(Z_f, Z_i, t) + Et)\right]. \quad (3-3)$$

B. Geometrical Meaning of the Amplitude Factor and the Maslov Index

Before proceeding, we examine very briefly the geometrical meaning of the amplitude factor in Eq.(3-3), particularly in the context of the periodic motion. Remembering Eq.(2-5), we investigate the meaning of the Jacobian determinant $\partial(Z_f - Z_i)/\partial Z_i$. This represents the sensitivity of the motions of an infinitesimal volume element in phase space to its initial location. It is required in quantum mechanics to think about the behavior not only of each phase space point but also of an volume element around it. Basically there are three kind of motions made by an infinitesimal volume element while carried by classical phase flow; (1)translation

(2)spinning around its own axis (3)deformation. The effect of the translation has already been removed out in the expression of $\partial(Z_f - Z_i)/\partial Z_i$. Thus only the internal motions, namely the spinning and deformations, should be considered.

Here we consider only an integrable case. For a heuristic and short discussion, we first imagine a one-dimensional harmonic oscillator. In Fig.1, a couple of infinitesimally nearby orbits are depicted, in which the coordinates are scaled so that the trajectories form complete circles. [Note that the distance between the two circles is exaggerated in the figure.] As the center of the tiny volume element ABCD moves along the trajectory, it only spins around its own axis with no deformation in this exceptionally ideal case. Thus the factor $\partial(Z_f - Z_i)/\partial Z_i$ in this case is just due to the spinning motion. Furthermore, it is quite simple to show that

$$\partial(Z_f - Z_i)/\partial Z_i = 4\sin^2\left(\frac{\omega_h t}{2}\right), \quad (3-4)$$

where ω_h is the frequency of the oscillator and is identical with that of the spin. $\omega_h t$ corresponds to b_k of Eq.(3-3). From this expression including the sine function, it is observed that the spinning motion generates an extra quantum phase in addition to the action. Because of the dividing factor 2 in Eq.(3-4), the progress of the phase due to the spinning motion is two times slower than that of the oscillator itself. This is essentially due to the square root in Eq.(2-4), which characterizes quantum mechanics.

If the oscillator is not harmonic, the trajectories deviate from the complete circles and thus the volume element deforms from time to time. However, as far as the volume element is confined to be infinitesimal, the effect of the deformation in $\partial(Z_f - Z_i)/\partial Z_i$ cannot be virtually observed at the every instance when the periodic motion is completed. This is simply because the volume element comes back to the original position, with the same orientation and shape at this particular instance. Further, Eq.(3-4) holds in this case, too. Thus again only the spinning motion can generate the additional quantum phase.

It is almost trivial to see that the above observation can be applied to multi-dimensional integrable systems, since the existence of the action-angle variables means that the total phase space can be viewed essentially as a direct product of independent two-dimensional phase spaces. On the other hand, in chaotic cases, the change of the shape after each iteration of the periodic motion is significantly large in general, and hence the phase change due to this deformation must be very important, as will be seen later.

There can be various ways of interpreting the physical or geometrical meaning of the Maslov index.¹⁵ In the DCF formalism, as is seen later, the continuous quantum phase due to the spinning motion brings about the Maslov index. This is in harmony with the current idea due to Littlejohn,¹⁶ who considers the Maslov index as a result of the continuous phase progress occurring in the representation of the so-called metaplectic operator in his semiclassical theory, and is quite different from the standard interpretation in the WKB theory, in which the sudden change of the phase by π is introduced whenever two wave functions based on the solutions of the Hamilton-Jacobi equation in different branches are patched together.^{15,17}

C. Manifolds Composed of Periodic Orbits

Let us reconsider the δ function in Eq.(3-3), which requires periodic orbits. Since Z_f is a function of Z_j , it is more appropriate to transform the δ function in the following form;

$$\delta(Z_f - Z_i) = \left| \partial(Z_f - Z_i) / \partial Z_j \right|^{-1} \delta(Z_i - Z_p(t)), \quad (3-5)$$

where $Z_p(t)$ denotes a point on a manifold which is composed of periodic orbits having the period t . Note that $Z_p(t)$ is a symbolic expression in that if $Z_p(t)$ is not a point (definitely it is not), the averaging procedure is understood to be taken implicitly. For example, in the action-

angle variables, the right hand side of Eq.(3-5) is not a function of the angle variables and consequently it should be divided by 2π for each dimension. Equation (3-5) thus reforms Eq.(3-3) as

$$D(E) = (\pi\hbar)^{-1} Re \int_0^\infty dt \int dZ_i \delta(Z_i - Z_p(t)) \prod_{k=1}^N \left(2i \sin\left(\frac{b_k}{2}\right)\right)^{-1} \times \exp\left[\frac{i}{\hbar}(S(Z_t, Z_i, t) + Et)\right]. \quad (3-6)$$

Unlike the Gutzwiller's theory, Eq.(3-6) includes the (stability) component for the direction of the periodic motion among b_k 's, which should have the form of ωt , where ω is the frequency of the total periodic motion, as shown in the preceding subsection. This makes the inverse sine function here become infinity at each instance when the periodic motion is completed. However, from the other parts of the integral, zero value arises unless a certain condition is not fulfilled. Thus we have spikes only at specific energies, as will be seen in the following sections.

IV. INTEGRABLE SYSTEMS (THE EBK CONDITIONS)

For integrable systems, the EBK conditions are perfectly established both theoretically and numerically. The relationship between the EBK and the periodic orbit theory has been studied extensively by Berry and Tabor.⁴ Physically, a single periodic orbit does not cover an entire torus, while a multiply periodic orbit does. Logically, therefore, it seems not obvious that the EBK conditions can be derived within the periodic orbit scheme. Very recently, Ozorio de Almeida¹⁸ has given a very interesting and delicate answer to this question; the tori

composed of periodic orbits which lie arbitrarily close to the quantized torus makes phase-coherent contributions to the sum formula. I would like to show another possibility of understanding it, by relaxing the strict periodic-orbit condition, which was mentioned earlier below Eq.(3-2). Through this relaxation, the multiply periodic orbits in the vicinity of the original periodic orbit are taken into account. The reader can skip this section if not interested in the regular spectrum.

A. The Strict Periodic Orbit Condition

We first write down the δ function in Eq.(3-6) in terms of action variables. For a one dimensional case this is

$$\delta(Z - Z_p(t)) = (2\pi)^{-1} \sum_r \int d(rT) \delta(I - I^0(T)) \delta(t - rT), \quad (4-1)$$

where $I^0(T)$ is an action variable having the period T and r is the rotation number. So, t has to coincide with one of rT , T being, in turn, a function of I . It is extended to a multidimensional case in a straightforward way such that

$$\delta(Z - Z_p(t)) = (2\pi)^{-N} \sum_{n=-\infty}^{\infty} \prod_{k=1}^N \sum_{r_k} \left[\int d(n r_k T_k) \delta(I_k - I_k^0(T_k)) \delta(t - n r_k T_k) \right]. \quad (4-2)$$

Each action variable I_k is associated with the frequency $\omega_k (= 2\pi/T_k)$. Let a vector R correspond to the topology of a periodic orbit by assigning its k -th component with r_k , which is the rotation number in the direction of θ_k (that is $\theta_k = 2\pi r_k$) in a single circuit of the *total* periodic motion. The total period T_R is simply given by $r_k T_k$ for any k . The number n in

Eq.(4-2) is the number of rotations of such a total periodic motion. The product of δ functions including t can be rewritten for $n = 1$, for instance, as

$$\delta(t - r_k T_k) \delta(r_1 T_1 - r_2 T_2) \delta(r_2 T_2 - r_3 T_3) \cdots \delta(r_{N-1} T_{N-1} - r_N T_N), \quad (4-3)$$

where these $N-1$ commensurable relations clearly require the orbit to be periodic. We bring Eqs. (4-2) and (4-3) back into Eq.(3-6), and integrate over all the variables except I_J and T_J , which gives

$$D(E) = (2\pi\hbar)^{-1} \sum_{\mathbf{R}} \sum_{n=-\infty}^{\infty} \int dI_1 \int d(nr_1^{\mathbf{R}} T_1) \prod_{k=1}^N \left(2i \sin \left(\frac{nb_k^{\mathbf{R}}}{2} \right) \right)^{-1} \\ \times \delta(I_1 - I_1^0(T_1)) \exp \left[\frac{i}{\hbar} n \left(2\pi \sum_k r_k^{\mathbf{R}} I_k - H(I) T_R + E T_R \right) \right], \quad (4-4)$$

where the sum over the topology \mathbf{R} is meant by the original expression in Eq.(4-2), and the element of vector \mathbf{R} is specified by the superscript R . The stability components b_k in Eq.(4-4) are redefined so that they are evaluated for each single circuit of the periodic motions, and are thus different from those of Eq.(3-6).

The reason why the integration over (T_J, I_J) plane is left undone is that we are going to relax the strict periodic condition in the next step to take account of the trajectories surrounding the periodic orbit. This procedure can be made for any (T_k, I_k) pair with $k=1, 2, \dots, N$. In fact, we will see that the final quantum condition to be obtained does not depend on the choice of the pair. This is simply because the periodic orbit is stable in any direction. On the other hand, the situation is quite different if the system is in chaos and we will see this in the next section.

B. Relaxation of the Strict Periodic Orbit Condition

Up to Eq.(4-4), the trajectories considered in the integrand have been determined in such a way that: (i) The total length of the running time is $T_R = nr_I^R T_I$, (ii) All the action variables are fixed except for I_J , which is left as a variable. Setting $I_1 = I_1^0(T_1)$, of course, leads to a periodic orbit. Only after these integral processes, the periodic orbits considered in Eq.(4-4) can be deformed continuously to non-periodic orbit by varying I_J , as long as the total running time $nr_I^R T_I$ is fixed. Note that the frequencies $\omega_{k's}$ ($k \neq 1$) depend on I_J , too. In order to introduce such relaxation, we replace the δ function for I_J with a smoothed function, keeping both the topology R and time T_I fixed (this means that total time T_R is fixed accordingly). We choose this replacing function to be the simplest one, that is a square function, the width of which is \hbar/r_1 , with the center being $I_1^0(T_1)$, and the height is r_1/\hbar . Outside the square, the function is set to be zero. The reason to take this width is that the phase in Eq.(4-4) covers the range of at least 2π as I_J is varied by unity, so that the stationary phase approximation makes sense. In the classical limit of $\hbar \rightarrow 0$, this square function goes back to the δ function. On the other hand, we have no *a priori* reason, other than its simplicity, why the square function has to be chosen. This is a drawback and needs further study on what happens if the other functional forms are used.

After all, $D(E)$ is evaluated in the following order: (1) I_J -integration fixing T_I . As in the usual application of the stationary phase approximation, the integration range is essentially extended to minus and plus infinities. The stationary phase point is found to be located at $I_1 = I_1^0(T_1)$, which is the original periodic orbit. In reality, if this were not the case, the replacement of the δ function had been invalid. Thus, the major contribution has been found in the periodic orbits in spite of the removal of the strict periodic orbit condition. We here *assume* the existence of such periodic orbits. (2) T_I -integration. The stationary phase condition requires that the energy of the classical trajectory must be identical with E of $D(E)$. The most parts of the

amplitude factors in the stationary phase approximations for the two coordinates cancel each other [see Eq.(5-3) for essentially the same argument], and the integrated value turns out to be

$$D(E) = \frac{1}{\hbar} \sum_R \frac{T_R}{2\pi} \sum_{n=-\infty}^{\infty} \prod_{k=1}^N \left(2i \sin \left(\frac{n b_k^R}{2} \right) \right)^{-1} \exp \left[\frac{i}{\hbar} 2\pi n \sum_j^N r_j^R I_j^0 \right]. \quad (4-5)$$

Obviously, the stationary phase approximation in T_I coordinate is not valid at all for $n = 0$. This case corresponds to the Thomas-Fermi density and has been analyzed in a great detail by Berry and Mount.¹⁹ Nonetheless, we include the case of $n = 0$ just in the above formal sense. It should be noted that although we had relaxed the strict periodic orbit condition only in (T_I, I_I) coordinates, Eq.(4-5) appeared not to depend on this particular choice. This means that the same procedure can be performed on the other (T_k, I_k) coordinates with the same result. This situation is peculiar to integrable systems.

As usual, making use of the following identity^{3b}

$$\left(2 \sin \left(\frac{n b_k}{2} \right) \right)^{-1} = i \sum_{m_k=0}^{\infty} e^{-i \left(m_k + \frac{1}{2} \right) n b_k} \quad (4-6)$$

where $b_k^R = r_k^R \omega_k T_k$, and of the Poisson sum formula²⁰ we get

$$\begin{aligned} D(E) &= \sum_R \frac{T_R}{2\pi} \sum_{M=-\infty}^{\infty} \sum_{m_1=0}^{\infty} \sum_{m_2=0}^{\infty} \cdots \sum_{m_N=0}^{\infty} \delta \left(\sum_{k=1}^N r_k^R \left\{ I_k^0 - \left(m_k + \frac{1}{2} \right) \hbar \right\} - M \hbar \right) \\ &= \sum_R \sum_{M=-\infty}^{\infty} \sum_{m_1=0}^{\infty} \sum_{m_2=0}^{\infty} \cdots \sum_{m_N=0}^{\infty} \delta \left(E - E \left[W_R = \sum_k^N \left(m_k + \frac{1}{2} \right) \hbar + M \hbar \right] \right), \end{aligned} \quad (4-7)$$

where W_R is Hamilton's characteristic function, whose partial derivative by E is T_R . The summation over M is redundant here, and thereby

$$D(E) = \sum_R \frac{T_R}{2\pi} \sum_{m_1=0}^{\infty} \sum_{m_2=0}^{\infty} \cdots \sum_{m_N=0}^{\infty} \delta \left(\sum_k^N r_k^R \left\{ I_k^0 - \left(m_k + \frac{1}{2} \right) \hbar \right\} \right). \quad (4-8)$$

If a system at hand has periodic orbits satisfying all the stationary phase conditions under the given topology, then Eq.(4-8) leads to a quantum condition

$$\sum_k^N r_k^R \left\{ I_k^0 - \left(m_k + \frac{1}{2} \right) \hbar \right\} = 0, \quad (4-9)$$

which should be quoted as the resonant quantum condition, since the periodic orbit is essentially resonant orbit in the sense that the commensurable relations as in Eq.(4-3) holds. In this case, the action variables are not calculated individually but only in the form of linear combinations, namely $\sum r_k^R I_k^0$. Accordingly, the Maslov index is not 2 any more.

On the other hand, when the system does not have such rigorous periodic orbits on the energy shell required, we should have approximated the stationary phase evaluation of Eq.(4-4) with use of a multiply periodic orbit, which is supposed to come back to a point arbitrarily close to the original point after the time T_R . Such introduction of the multiply periodic orbits has been made possible by the relaxation of the strict periodic orbit condition, and the error expected in this approximation to the stationary phase approximation must be arbitrarily small. In introducing multiply periodic orbits into the theory, we have to modify the idea about the period and topology: A rigorous periodic orbit does not change its topology and period throughout the periodic motion. On the other hand, in case of multiply periodic orbit, the topology and the period can be identified only as a result that the orbit has been realized to come back to a point very close the original point. The topology and period can change in each

quasi-circuit. Moreover, a single multiply periodic orbit is assumed to generate all the linearly independent topologies \mathbf{R} eventually. This is of course due to the incommensurable relations among the frequencies, and recently this idea has been applied numerically by Mehta and De Leon.²² Once this situation has been taken into account, the mathematical procedure from Eq.(4-5) to (4-8) is the same as before. Thus Eq.(4-9) reads that a vector, the k -th component of which is $I_k^0 - \left(m_k + \frac{1}{2}\right)\hbar$, is orthogonal to all the independent vectors \mathbf{R} . Hence, a single (multiply periodic) orbit can satisfy the conditions like Eq.(4-9) only when it holds that

$$I_k^0 = \left(m_k + \frac{1}{2}\right)\hbar \quad (k = 1, \dots, N), \quad (4-10)$$

which are the EBK conditions. In the intermediate case where the resonance in the above sense occurs partly, Eq.(4-9) and Eq.(4-10) should be combined together.

V. UNSTABLE SYSTEMS

A. General Expression of $D(E)$

In this section, we assume that all of the b_k 's are complex with one exception that corresponds to the parallel direction to the periodic motion. In a phase space, periodic orbits form a one parameter family (a curved plane) which intersects transversally with the constant energy surfaces.²³ Let I be a coordinate on this plane which intersects vertically with each periodic orbit. The coordinate I is essentially equivalent to an action variable. Accordingly, the coordinate along each periodic orbit is named θ . Then we introduce a set of local coordinates along (I, θ) , which is $\{u_k(\theta, I_\alpha^0), k=1, 2, \dots, 2N-2\}$, and in particular, a point $\{u_k^0(\theta, I_\alpha^0)\}$ is supposed to locate on the periodic orbit. This coordinate transformation in phase space can be

area-preserving, the explicit form of which is not necessary at all for our purpose. The δ function in Eq.(3-6) for the periodic manifold is then written as

$$\delta(Z - Z_p(t)) = (2\pi)^{-1} \sum_{\alpha} \sum_{n=-\infty}^{\infty} \int d(nT_{\alpha}) \delta(t - nT_{\alpha}) \delta(I_{\alpha} - I_{\alpha}^0(T_{\alpha})) \times \prod_{k=1}^{2N-2} \delta(u_k - u_k^0(\theta, I_{\alpha}^0)). \quad (5-1)$$

As in the integrable case, Eq.(5-1) can be integrated directly for all the coordinates except for I and θ , the result being

$$D(E) = (2\pi \hbar)^{-1} \sum_{\alpha} \sum_{n=-\infty}^{\infty} \int dI_{\alpha} \int d(nT_{\alpha}) \prod_{k=1}^N \left(2i \sin \left(\frac{n b_k^{\alpha}}{2} \right) \right)^{-1} \times \delta(I_{\alpha} - I_{\alpha}^0(T_{\alpha})) \exp \left[\frac{i}{\hbar} (S_{\alpha}(\eta_i, \eta_i, nT_{\alpha}) + nET_{\alpha}) \right]. \quad (5-2)$$

In what follows, the stability factors b_k^{α} ($= d_k^{\alpha} + ic_k^{\alpha}$) bear the superscript α to specify the periodic orbit, only when necessary.

Here again the strict periodic-orbit condition is relaxed. Just as in the preceding section, we replace the δ function with a square function, of which height is \hbar and width is $1/\hbar$ with the center at $I_{\alpha}^0(T_{\alpha})$. Among the δ functions for various coordinates in Eq.(5-1), such relaxation is allowed only in I coordinate, since the instability of the periodic orbit makes no sense of the idea of "contact vicinity of the original orbit" in the other coordinates. On the other hand, the family of the periodic orbits is stably arranged in the I direction. An integrable system allows this sort of relaxation to every direction of the action variables, since a periodic orbit in this case is surrounded by stable vicinity in the all directions. Except for this difference, the periodic orbit theory can treat both integrable and non-integrable cases on the equal theoretical

basis. In this way, we apply the stationary phase approximation only in the I coordinate. On the other hand, the trace formula in Gutzwiller's theory¹ takes the q -coordinates (configuration space) for the stationary phase approximation regardless of the topological arrangement of periodic orbits. Since the present theory think about the vicinity of the periodic orbit in phase space, in which the stable manifold composed of the periodic orbits as a one-parameter family can be clearly identified, our trace operation seems more natural.

As in the integrable case, the stationary phase approximation is applied as follows. (1) I_α -integration with the extended domain of the integration (actually the infinite one). The stationary phase point is found to be located at $I_\alpha^0(T_\alpha)$ and we have

$$D(E) = (2\pi\hbar)^{-1} \sum_{\alpha} \sum_{n=-\infty}^{\infty} \frac{1}{\omega_{\alpha}\hbar} \int d(nT_{\alpha}) \prod_{k=1}^N \left(2i \sin\left(\frac{n b_k^{\alpha}}{2}\right) \right)^{-1} \left(\frac{2\pi i \hbar}{\frac{\partial T_{\alpha}}{\partial I_{\alpha}}} \right)^{1/2} \\ \times \exp\left[\frac{i}{\hbar} (S_{\alpha}(\eta_i, \eta_i, nT_{\alpha}) + nET_{\alpha})\right]. \quad (5-3)$$

Here, the partial derivative $\partial T_{\alpha} / \partial I_{\alpha}$ due to the stationary phase evaluation is understood to be taken at the given values of T_{α} and I_{α} . (2) In T_{α} -integration, the stationary phase condition requires that the energy of the classical trajectory must be equal to E of $D(E)$. Furthermore some cancellation in the amplitude factors occurs leaving a simple result as

$$D(E) = \frac{1}{\hbar} \sum_{\alpha} \sum_{n=-\infty}^{\infty} \frac{1}{\omega_{\alpha}} \prod_{k=1}^N \left(2i \sin\left(\frac{n b_k^{\alpha}}{2}\right) \right)^{-1} \exp\left[\frac{i}{\hbar} n W_{\alpha}(\eta_i, \eta_i, E)\right]. \quad (5-4)$$

Here again, the stationary phase approximation for $n = 0$ has been carried out formally.

In order to remember that b_k 's are generally complex, we denote them as in Eq.(2-9).

In expanding the inverse sine function of Eq.(5-3), we have two possibilities, namely

$$\left\{2i \sin\left(\frac{nb_k}{2}\right)\right\}^{-1} = \sum_{m_k=0}^{\infty} e^{-i\left(m_k+\frac{1}{2}\right)nb_k} \quad \text{for } nc_k \geq 0 \quad (5-5a)$$

or

$$\left\{2i \sin\left(\frac{nb_k}{2}\right)\right\}^{-1} = \sum_{m_k=0}^{\infty} e^{i\left(m_k+\frac{1}{2}\right)nb_k} \quad \text{for } nc_k < 0. \quad (5-5b)$$

These expansions are both convergent. As stated in the last part of Sec.II, our convention of choosing the roots of ib_k 's on the B-plane, nc_k is always selected to be positive, that is $ib_k = n(c_k + id_k)$ for $n > 0$ and $ib_k = n(-c_k + id_k)$ for $n < 0$, and hence we only use Eq.(5-5a) under this circumstance. (Equation (5-5b) might be required in the other convention.) Putting these into Eq.(5-4) and applying the Poisson sum formula,²⁰ we obtain our final result

$$D(E) = \sum_{\alpha} \frac{T_{\alpha}}{2\pi} \sum_{M=-\infty}^{\infty} \sum_{m_1=0}^{\infty} \sum_{m_2=0}^{\infty} \cdots \sum_{m_N=0}^{\infty} \left[\frac{i}{W_{\alpha} - \hbar \sum_{k=1}^N \left(m_k + \frac{1}{2}\right) d_k^{\alpha} - 2\pi M \hbar + i\hbar \sum_{k=1}^N \left(m_k + \frac{1}{2}\right) |c_k^{\alpha}|} - \frac{i}{W_{\alpha} - \hbar \sum_{k=1}^N \left(m_k + \frac{1}{2}\right) d_k^{\alpha} - 2\pi M \hbar - i\hbar \sum_{k=1}^N \left(m_k + \frac{1}{2}\right) |c_k^{\alpha}|} \right] \quad (5-6)$$

The first term in the square bracket comes from the positive time ($n \geq 0$), whereas the second one is due to the negative time ($n < 0$). In the genral case (see Table I), both $|d|$ and $-|d|$ appear at the same time in the denominator in the above expression. (The cases of hyperbolic

fixed points are exceptions.) So, if the quantum numbers associated with $|d|$ and $-|d|$ happen to be mutually equal, these terms are cancelled out in the denominators.

Equation (5-6) can be converted very easily into the form of the "Lorentzian",¹ that is

$$D(E) = \sum_{\alpha} \frac{T_{\alpha}}{2\pi} \sum_{M=-\infty}^{\infty} \sum_{m_1=0}^{\infty} \sum_{m_2=0}^{\infty} \cdots \sum_{m_N=0}^{\infty} \frac{2\hbar \sum_{k=1}^N \left(m_k + \frac{1}{2}\right) |c_k^{\alpha}|}{\left[W_{\alpha} - \hbar \sum_{k=1}^N \left(m_k + \frac{1}{2}\right) d_k^{\alpha} - 2\pi M \hbar \right]^2 + \left[\hbar \sum_{k=1}^N \left(m_k + \frac{1}{2}\right) |c_k^{\alpha}| \right]^2}. \quad (5-7)$$

This expression is an extension of Gutzwiller's one¹ in that (i) the "quantum numbers" m_k are correctly treated (in Gutzwiller's theory, all the quantum numbers except for M and one corresponding to the direction of the periodic motion are fixed to be zero^{6a}), (ii) all the quantum numbers corresponding to any directions are treated on an equal footing (note that at least one of c_k 's in the above expression is exactly zero, which should correspond to the direction of the periodic motion.) (iii) the dimensionality is not restricted (if we consider a two dimensional system having a simple hyperbolic fixed point, for which $d_k = 0$, Eq.(5-7) reproduces Gutzwiller's Eq.(44) of his paper in J. Math. Phys. (1971)). The meaning of the "quantum numbers" is discussed below.

VI. DISCUSSION

A. Weakly Unstable and Stable Non-integrable Systems

$D(E)$ is essentially the sum of the Lorentzian curves each of which is generated by a periodic orbit α . To see this more clearly, we expand W_α in the energy and take it up to the first order, which results in

$$D(E) = \frac{1}{\pi} \sum_{\alpha} \sum_{M=-\infty}^{\infty} \sum_{m_1=0}^{\infty} \sum_{m_2=0}^{\infty} \cdots \sum_{m_N=0}^{\infty} \quad (6-1)$$

$$\frac{\hbar}{T_\alpha} \sum_{k=1}^N \left(m_k + \frac{1}{2}\right) |c_k^\alpha|$$

$$\left[E - E_\alpha + \left\{ W_\alpha(E_\alpha) - \hbar \sum_{k=1}^N \left(m_k + \frac{1}{2}\right) d_k^\alpha - 2\pi M \hbar \right\} / T_\alpha \right]^2 + \left[\frac{\hbar}{T_\alpha} \sum_{k=1}^N \left(m_k + \frac{1}{2}\right) |c_k^\alpha| \right]^2$$

where E_α is a quantized energy which makes the curly bracket of Eq.(6-1) zero under a certain set of "quantum numbers", and E is supposed to be close to E_α . Further, it was assumed here that the energy dependence of c_k 's and d_k 's are much smaller within the width. The width is the sum of the instability factors of all the directions transversal to the periodic motion, each of which is associated with the "quantum numbers". Remember again that the stability components b_k in Eqs.(5-7) and (6-1) are taken for each single circuit of the periodic motion (not accumulated).

Naturally, a periodic orbit having at least one large instability component $|c_k^\alpha|/T_\alpha$ cannot have a sharp peak. If $|c_k^\alpha|/T_\alpha$ is moderately large, but not too large, the Lorentzian can have a significant peak only when m_k is zero. This is the case considered by Gutzwiller.¹ However, on the transition from a stable (or an integrable) to strongly unstable case, there can exit a weakly unstable one having only small $|c_k^\alpha|/T_\alpha$'s, which can support even "excited states" or the states of non-zero quantum numbers associated with c_k . Therefore, neglecting these

quantum numbers can lead to wrong assignment of the spectroscopy and to bad estimate of the nearest-neighbor level spacing. Currently, we have no general rule or tendency of the relationship between the magnitude of c_k and the period T_α . It is conceived qualitatively, however, that the longer becomes the period, the larger c_k 's grow. In this regard, it is important to note that unstable periodic orbits with long periods should not be excluded under a simple minded idea that they must have large instability factors. Conversely, it is not correct either to conclude that only periodic motions having very long periods can contribute to the high resolution of energy spacing.

Let us examine a limiting case of Eq.(5-7), where all the instability components c_k 's become zero. The fact that all the quantum numbers are treated on equal footing in Eqs.(5-7) and (6-1) is very helpful for smooth change from the expression of an unstable case to that of a stable one. It simply becomes

$$\lim_{c_k \rightarrow 0} D(E) = \sum_{\alpha} T_{\alpha} \sum_{m_1=0}^{\infty} \sum_{m_2=0}^{\infty} \cdots \sum_{m_N=0}^{\infty} \delta \left(W_{\alpha} - \sum_{k=1}^N \left(m_k + \frac{1}{2} \right) d_k^{\alpha} \hbar - 2\pi M \hbar \right) \quad (6-2)$$

which has the same form as Eq.(4-7), and will lead to the resonant type quantum condition (not the EBK for multiply periodic orbits). Thus $D(E)$ in an unstable case has been shown to have the sound limit. Strictly speaking, however, the expression in Eq.(6-2) is more general than that in Eq.(4-7) in that the former does not assume the existence of the action-angle variables, namely the integrability, but simply assuming the zero instability ($c_k = 0$). Thus Eq.(6-2) can be applied to a stable but non-integrable system.

The above consideration leading to Eq.(6-2) helps to understand the role of the "quantum numbers" m_k in quantum chaos. In the limit to the stable case, these numbers correspond to the quantum numbers in the resonant quantum condition, Eq.(4-9). It is obvious there that each quantum number m_k cannot necessarily have independent meaning, since only

the sum of $r_k(m_k+1/2)$ is the really required quantity. (Note that both r_k and m_k are integers and there can be more than one set of m_k 's to reproduce the same value of the sum of $r_k(m_k+1/2)$. This is in clear contrast to the quantum numbers in the EBK conditions. In the same sense, a single Lorentzian in Eq.(5-7) can have plural sets of quantum numbers within a required resolution, which leads to "accidental degeneracy" of the levels and thereby yields a high density around zero in the distribution of nearest-neighbor level spacing.

More importantly, $D(E)$ is the sum of all the possible periodic orbits, the number of which is expected to be enormous even in a single energy plane. For this reason and due to the possible accidental-degeneracy mentioned above, the assignment of the quantum numbers in most of the irregular spectra should be prohibitively difficult in general. This does not mean immediately, however, that no spectra in chaotic region are associated with quantum numbers. On the contrary, it is predicted that there may exist an weakly chaotic spectra for which the assignment is possible. In fact, Malta has reported very recently that there is a system in which $D(E)$ happens to be dominated by a single periodic orbit.⁷ If, further, there is no accidental degeneracy, the quantum numbers could be assigned approximately.

B. The Endurance Time in Decay of Quantum Time-Correlation Function

As seen in Eq.(6-1), only those periodic orbits whose width is smaller than some critical value of the energy level spacing (ΔE) can contribute to the density of states. This leads to an inequality

$$\frac{\hbar}{T_\alpha} \sum_{k=1}^N \left(m_k + \frac{1}{2}\right) |c_k^\alpha| \leq \Delta E. \quad (6-3)$$

In order to specify a stationary state in terms of periodic orbits, the experimental setting should be longer than at least T_α , but, on the other hand, $\sum (m_k + \frac{1}{2}) |c_k^\alpha|$ tends to deteriorate the identity of the vicinity of the periodic orbit. These two factors thereby compete each other. Thus we define the endurance time by

$$\tau_\alpha = \frac{T_\alpha}{\sum_{k=1}^N (m_k + \frac{1}{2}) |c_k^\alpha|} . \quad (6-4)$$

If the endurance time is shorter compared to a possible measuring time such as the life-time of photo-emission, such an experiment cannot determine whether α takes part in supporting an eigenstate. In an integrable case, the endurance time is infinite (the period T_α is finite though), which allows a practical determination of the eigenstates.

Of course, the above argument on the observability of each chaotic eigenstate cannot be justified from any view point that the mathematical procedure to calculate Eq.(3-1) is purely equivalent to the eigenvalue problem of the Hamiltonian, which should not care about experimentally observing processes. In fact, Berry,²⁵ Voros,²⁶ and Eckhardt²⁷ have considered about how to get the fully resolved eigenvalues. One important point to note in this regard is that the semiclassical theory for $D(E)$ goes back to the time-dependent problem of dynamics where the mechanism of exponential decay due to "classical" chaos is automatically introduced (see below and also Eq.(3-1)), while the time-independent Schrödinger equation has been derived under the definite assumption of the existence of stationary states. At the present moment, I have no conclusion as to whether the semiclassical argument based on the phase space structure of classical mechanics is really relevant to the experiment to identify pure quantum states.

In order to see the physical meaning of the endurance time in a little greater detail, we Fourier-transform the quantized density of states of Eq.(6-1) back into the time domain, under the condition that one can find a set of quantum numbers which can make the curly bracket in the denominator of Eq.(6-1) become zero. Although the Lorentzian form is valid only where E is close to E_α , the integral domain is extended to the entire space, since the major contribution comes from only the vicinity of E_α anyway. Thus we have

$$\int_{-\infty}^{\infty} dE D(E) e^{-iEt/\hbar} = \int_{-\infty}^{\infty} dq \langle q | e^{-iHt/\hbar} | q \rangle \approx \sum_{\alpha} \exp\left[\frac{i}{\hbar} E_{\alpha} t - \frac{|t|}{\tau_{\alpha}}\right], \quad (6-5)$$

where E_α here is specified by the quantum numbers implicitly. The second and third terms in the above expression mean that the trace of the auto-correlation of quantum states is represented by the sum of the exponential decays superimposed by the oscillating features.

Recently, Heller has found an exponential decay in the long time behavior of the time correlation function of a Gaussian wave packet evolved along a periodic orbit.^{14a} His correlation function shows additional oscillating behavior due to the fact that the wave packet is a Gaussian-type superposition of energy eigenfunctions. Although the assumption that a Gaussian packet retains to be Gaussian^{14a} even under strong chaos and even for a long time seems quite hard to justify, Eq.(6-5) hereby supports the basic validity of his argument from a different point of view.

The exponential decay shown in Eq.(6-5) seems to expose an inherent difficulty of semiclassical theory in treating quantum chaos, since pure quantum treatment should not have such decaying factors irrespective of whether the spectrum of a system is regular or not. This difficulty arises because only the exponential separation of the nearby orbits from a periodic orbit is emphasized. The fact is that new trajectories enter into the close vicinity of a periodic

orbit after the predecessors have left and/or they are leaving. Besides, there is no absolute origin in time for bound-state problems. Hence, in addition to Eq.(6-5),

$$\int_{-\infty}^{\infty} dE D(E) \exp\left[\frac{-iE(t-t_0)}{\hbar}\right] \approx \sum_{\alpha} \exp\left[\frac{i}{\hbar} E_{\alpha}(t-t_0) - \frac{|t-t_0|}{\tau_{\alpha}}\right], \quad (6-6)$$

is also acceptable as a time-correlation function. Here t_0 is an arbitrary constant, at which the nearby orbits start to correlate with periodic orbits. By preparing many of these correlation functions and taking their sum extended in the entire time domain, we can construct conceptually an effective correlation-function which decays locally around the individual time origin t_0 but does not decay globally.

As an important consequence of this consideration, we are led to the following model of the behavior of classical trajectories: First of all, a phase-space structure is characterized by the set of periodic orbits, which are completely stationary. A non-periodic orbit wanders around in phase space migrating from the vicinity of one periodic orbit to that of another from time to time. If a trajectory sticks closely to some of periodic-orbits for a significantly long time, its behavior would look like an intermittency-type chaos. In fact, the present author has numerically observed a very typical intermittency clearly represented in terms of what we call quasi-action variable,²⁸ which is an extension of the action variable and yet has a natural generalization even in chaotic region. In order for a trajectory to support a bound state by staying in the close vicinity of a periodic orbit α , it should remain there for at least the period T_{α} . On the other hand, the trajectory is destined to leave from the vicinity according to the exponential decay as in Eq.(6-6), where t_0 is regarded as a time when the trajectory has come in the vicinity. Here we hypothesize that trajectories visit each periodic orbit with almost equal chances (democratically). Then the probability (denoted by p_{α}) for the close vicinity of α to be

occupied by non-periodic trajectories and to support bound state(s) with this occupation must be proportional to

$$(p_\alpha \propto) \exp\left[-\frac{T_\alpha}{\tau_\alpha}\right] = \exp\left[-\sum_{k=1}^N \left(m_k + \frac{1}{2}\right) |c_k^\alpha|\right]. \quad (6-7)$$

These are simply normalized so that their sum becomes equal to unity, that is

$$p_\alpha = \exp[A] \exp\left[-\sum_{k=1}^N \left(m_k + \frac{1}{2}\right) |c_k^\alpha|\right] \quad (6-8a)$$

with

$$A = -\ln \sum_{\alpha} \left[\exp\left(-\sum_{k=1}^N \left(m_k + \frac{1}{2}\right) |c_k^\alpha|\right) \right]. \quad (6-8b)$$

This is a modified version of the ergodic hypothesis which is relevant to quantum chaos. In the original ergodic hypothesis due to Boltzmann, the hypothetical existence of a trajectory which eventually visits every point of an energy plane leads to the equivalence between ensemble (phase-space) and time averages. Obviously, number of periodic orbits embedded in the energy plane, which plays the main role in the periodic orbit theory, work as the counter example that do not cover the entire plane. Thus, the concepts of the ergodic hypothesis and the periodic orbit theory in chaos are not in harmony with each other in principle. Therefore, our newly proposed hypothesis has integrated them.

Since $1/\tau_\alpha$ corresponds to the rate of losing the information (memory) for the periodic orbit α , and hence, it can be defined as entropy gained during the period. We call $1/\tau_\alpha$ the Gutzwiller entropy (h_G^α) for α . The total entropy of the energy shell can be defined by the

average of these local entropies taken over the periodic orbits whose τ_α is longer enough to have the Lorentzian significantly sharp, that is

$$\langle h_G \rangle = \sum'_\alpha \frac{1}{\tau_\alpha} p_\alpha. \quad (6-9)$$

The prime over the symbol of summation is used throughout in the above sense. If all the m_k 's of Eq.(6-4) are zero, $\langle h_G \rangle$ is compatible with the KS-entropy h_{KS} in classical chaos that is a phase-space average of the local Liapounov exponents.^{12,24} Note, however, that for KS-entropy the phase-space average is not meant to be the average over periodic orbits but over the entire energy plane. In addition, the Liapounov exponent in classical chaos is not exactly equivalent to our $\sum |c_k|$, but it is calculated in practice with the step-wise "distance" of separation from nearby orbits^{12,24} since classical chaos is concerned about not only periodic but general orbits. If all m_k 's are not zero in a weakly unstable system, h_G should be modified so that the quantum numbers are taken into account.

C. The Number of Periodic Orbits and the Boltzmann Entropy

In this subsection, we attempt to estimate, very roughly, the Boltzmann entropy for a microcanonical ensemble in terms of the results of semiclassical dynamics developed so far in the present paper. This subsection is confined only to an unstable system. As before, E_α is a quantized energy specified by a set of quantum numbers, in particular, all of the quantum numbers in the unstable directions are assumed to be zero. Under this assumption, the peak positions described by Eq.(6-1) are uniquely defined by these sets of quantum numbers. Let us consider the density of states locally averaged over a small energy interval ΔE ,

$$\Omega(E) = \frac{1}{\Delta E} \int_{E-\Delta E/2}^{E+\Delta E/2} D(E) dE. \quad (6-10)$$

Usually $\Omega(E)$, rather than $D(E)$, is referred to as the density of states in statistical mechanics. We choose ΔE so that it covers most of the widths of the sharp Lorentzian curves represented in Eq.(6-1). Thus $\Omega(E)\Delta E$ is estimated roughly as

$$\Omega(E) \Delta E \approx \sum_{\alpha} 1 = \left(\begin{array}{l} \text{The number of periodic orbits} \\ \text{on the energy shell whose } \tau_{\alpha} \text{ is} \\ \text{longer than } \hbar/\Delta E \end{array} \right) \equiv n(E). \quad (6-11)$$

Hence, $n(E)$ is an implicit function of \hbar and ΔE . Needless to say, Eq.(6-11) does not necessarily mean that each periodic orbit supports a single eigenstates. By definition, the Boltzmann entropy S turns out to be

$$S = k \ln[\Omega(E) \Delta E] \approx k \ln(n(E)), \quad (6-12)$$

where k is the Boltzmann constant. Thus S has a simple relation to a dynamical quantity, which requires counting the number of the *eligible* periodic orbits in the sense of Eq.(6-11). In the classical limit ($\hbar \rightarrow 0$), all the periodic orbits on the energy shell can clear the eligibility. Moreover, since the Poincaré recurrence theorem assures that any orbit can be regarded as an arbitrarily close approximation to some periodic orbit, the above number counting can be replaced by the measure of the relevant volume element in classical phase space.

Let us try to define the local Boltzmann entropy just as the topological or dynamical entropies, such as h_{KS} and h_G , are defined first for an individual orbit. (Note that both h_{KS} and h_G have dimensions of the inverse of time.) For this purpose, we can take an advantage of the parallelism between statistical and quantum (and classical) mechanics : It is quite well-

known that from the analogy between the quantum time evolution operator $\exp[-iHt/\hbar]$ and the operator of the partition function $\exp[-\beta H]$ ($\beta = 1/k\mathbb{T}$), where \mathbb{T} indicates a temperature, β is regarded as an imaginary time, that is one can write formally that $t_{imag} = -i\hbar\beta$. Also we already have two standard classical equalities;

$$\frac{\partial W}{\partial E} = t \quad (6-13a)$$

$$\frac{\partial S}{\partial E} = k\beta . \quad (6-13b)$$

Again, W and S are Hamilton's characteristic function and the entropy, respectively. Now, let us go back to Eq.(5-6). In the positive-time component, $D(E)$ has a pole at

$$W_{\alpha}(E_{*}) = \hbar \sum_{k=1}^N \left(m_k + \frac{1}{2} \right) d_k^{\alpha} - 2\pi M \hbar - i\hbar \sum_{k=1}^N \left(m_k + \frac{1}{2} \right) |c_k^{\alpha}|, \quad (6-14)$$

where E_{*} indicates an energy corresponding to a pole in the complex energy plane. In analogy of Eq.(6-13a), the energy derivative of the complex-valued W_{α} should bring about a complex time as

$$\frac{\partial}{\partial E} W_{\alpha}(E_{*}) = T_{\alpha} - i\hbar \hat{\beta}_{\alpha}, \quad (6-15)$$

where T_{α} indicates the period again and

$$-i\hbar \hat{\beta}_{\alpha} = i \frac{\partial}{\partial E} \text{Im} [W_{\alpha}(E_{*})] = -i\hbar \frac{\partial}{\partial E} \sum_{k=1}^N |c_k^{\alpha}|/2, \quad (6-16)$$

[note $m_k=0$] and thus

$$\hat{\beta}_\alpha = \frac{\partial}{\partial E} \sum_{k=1} |c_k^\alpha|/2. \quad (6-17)$$

The quantity $\mathbb{T}_\alpha = 1/(k\hat{\beta}_\alpha)$ can be termed as the local temperature associated with the periodic orbit α , in light of the formal relation $t_{imag} = -i\hbar\beta$. Then, by comparing Eqs.(6-13b) and (6-17), we can define the local Boltzmann entropy such that

$$S_\alpha = -\frac{k}{\hbar} \text{Im} [W_\alpha(E^*)] + \text{const.} = k \sum_{k=1} |c_k^\alpha|/2 + \text{const.} \quad (6-18a)$$

Here the arbitrary constant in this expression is chosen to be zero, that is

$$S_\alpha = -\frac{k}{\hbar} \text{Im} [W_\alpha(E^*)] = k \sum_{k=1} |c_k^\alpha|/2. \quad (6-18b)$$

Since $\sum |c_k^\alpha|/2$ is regarded as information lost during the period, as described in Sec.VI.B, S_α thus defined is compatible with the concept of Shannon's information entropy. Connecting the local Boltzmann entropy with the imaginary part of Hamilton's characteristic function is not meaningless, since a relationship between statistical mechanics and resonance scattering theory and/or tunneling phenomena could be established.

It should be noted that we have started from Eq.(6-14), which corresponds to a pole of the positive-time part of $D(E)$ of Eq.(5-6). If, on the other hand, we begin with the negative-time component, namely

$$W_\alpha(E^*) = \hbar \sum_{k=1}^N \left(m_k + \frac{1}{2}\right) d_k^\alpha - 2\pi M \hbar + i\hbar \sum_{k=1} \left(m_k + \frac{1}{2}\right) |c_k^\alpha|, \quad (6-19)$$

the local entropy S_α becomes negative, and accordingly the temperature bears the opposite sign.

We next construct a total entropy of microcanonical ensemble. Let us remember the quantity p_α defined in Eq.(6-8a), which is the probability for the close vicinity of a periodic orbit α to be occupied by trajectories and to support bound state(s). Since all the m_k 's should be set to zero here, we have

$$p_\alpha = \exp[-A] \exp \left[- \sum_{k=1}^N |c_k^\alpha|/2 \right] = \exp[A] \exp[-S_\alpha/k] \quad (6-20)$$

with

$$A = - \ln \left[\sum_\alpha \exp[-S_\alpha/k] \right], \quad (6-21)$$

where S_α has been defined in Eq.(6-18b). It is noteworthy to confirm that the probability p_α is proportional to $\exp[-S_\alpha/k]$. With these probability functions the Gibbs entropy or Shannon's information entropy (denoted by S_{II}) is given by

$$S_{II} = -k \sum_\alpha p_\alpha \ln p_\alpha. \quad (6-22)$$

Or defining

$$\sigma_\alpha = -k \ln p_\alpha = S_\alpha - kA, \quad (6-23)$$

one can rewrite S_{II} as

$$S_{II} = \sum_{\alpha} \sigma_{\alpha} \exp\left[\frac{-\sigma_{\alpha}}{k}\right] = \sum_{\alpha} (S_{\alpha} - kA)p_{\alpha} = \sum_{\alpha} S_{\alpha}p_{\alpha} - kA. \quad (6-24)$$

As is well-known, it holds that

$$S \geq S_{II} \quad (6-25)$$

which means that S in Eq.(6-12) is the maximum for S_{II} . The equality holds as usual in case where all the S_{α} 's happen to be the same.

From Eq.(6-24), S_{II} is known to be composed of two pieces: The first sum in the right-most equality ($\sum_{\alpha} S_{\alpha}p_{\alpha}$) indicates the average of the local dynamical-entropies and bears a close connection to the Gutzwiller entropy defined in Eq.(6-9). The Gutzwiller entropy as well as h_{KS} represent a rate process of mixing in phase space and are of topological nature, while the Boltzmann entropy is usually supposed to represent the capacity of a microcanonical ensemble. The second term $-kA$ in Eq.(6-24) is of more statistical nature, since it just comes from the normalization condition. For instance, even if the dynamical part of S_{II} happens to be zero, namely $S_{\alpha}=0$ or $\sum |c_k^{\alpha}|/2 = 0$ for all α , which implies that the system under study is stable, A still have a non-zero value, actually that is equal to $\ln(n(E))$. Thus $-A$ is really viewed as the capacity of a microcanonical ensemble. On the other hand, as S_{α} 's become larger, $-A$ gets smaller, according to Eq.(6-21), and can turn out to be even negative. Also, the more becomes the number of periodic orbits, the more σ_{α} is dominated by $-A$, and thus S_{II} in a macroscopic system is expected to approach S . Further, from Eq.(6-23), σ_{α} can be regarded again as a local entropy in which the effect of the ensemble is taken into account.

Incidentally, the temperature is also predicted through S_{II} as

$$\beta = \frac{\partial S_{II}}{\partial E} = -\frac{1}{k} \sum_{\alpha} \left[\left(S_{\alpha} - \sum_{\gamma} S_{\gamma}p_{\gamma} \right) \beta_{\alpha} p_{\alpha} \right]. \quad (6-26)$$

Again, β is written in terms of the dynamical quantities. As seen in this expression, the contribution from each local entropy to the total β depends not only on the local β , which can be positive or negative, but also on magnitude of the local dynamical-entropy measured from their average.

As for the number of periodic orbits, by the way, there have been some theorems, in which the number of periodic orbits having a period T , denoted by $N(T)$, is given by

$$N(T) \approx C_1 \frac{\exp(h_{KS}T)}{T}, \quad (T \rightarrow \infty) \quad (6-27a)$$

or

$$N(T) \approx C_2 \exp(h_{KS}T), \quad (T \rightarrow \infty) \quad (6-27b)$$

where C 's are constants. The first estimate has been derived by Bowen^{29a} for the so-called axiom A flow (a geodesic flow on a compact manifold of constant negative curvature satisfying certain conditions),²⁹ and the second one is given by Zaslavsky et al.³⁰ for more general cases but on a less rigorous ground. Although there seems to be of no practical use, the logic leading to Eq.(6-28b) suggests that it had better be replaced by

$$N(T) \approx C_3 \exp(\langle h_G \rangle T), \quad (T \rightarrow \infty) \quad (6-28)$$

since $\langle h_G \rangle$ involves the information only of periodic orbits, while h_{KS} does not. If a method predicting $\langle h_G \rangle$ is available without actual search for the periodic orbits, Eq.(6-28) can be useful

for an estimate of the Boltzmann entropy, since knowing the Boltzmann entropy S of Eq.(6-12) is equivalent to knowing the number of eligible periodic orbits.

Although the discussion in this subsection is crude, the Boltzmann entropy has been described as a function of the instability components of the periodic orbits. Obviously, more rigorous discussion is required for these results to be clearly stated, even though accuracy required for the quantities of statistical mechanics or thermodynamics is generally much coarser than that for pure mechanics. Yet, one of the goals in the study of quantum chaos is to set a dynamical foundation for statistical mechanics.

VII. CONCLUDING REMARKS

We have examined the density of states both for regular and chaotic cases in a uniform manner from the view point of the phase-space periodic-orbit theory based on DCF. An extended expression of the density of states in chaotic regime has been obtained, and the roll of the "quantum numbers" has been discussed. Further, we have pointed out the possible existence of "excited states" with non-zero quantum numbers in unstable directions, if a system is weakly unstable. The quantum conditions for multiply periodic orbits and resonant ones in integrable systems (the EBK and its resonance version), and that for a stable non-integrable case have been discussed. Some insight into classical and quantum chaos has been obtained. Especially, the Liapounov exponent and Greene's residue in classical chaos have been derived from quantum mechanics in a natural manner. A very simple interpretation for the Maslov index has been given as well. All these three quantities are closely related to each other through the amplitude factor of the identity DCF. It has been attempted to connect some basic concepts of statistical mechanics with quantum chaos. The Boltzmann entropy for microcanonical ensemble has been described in terms of the number of periodic orbits.

The convergence problem adherent to the semiclassical theory, that is that the theory does not give δ function-like spikes for $D(E)$ in chaos, is not solved at all. Also, any practical method to calculate the state density has not been presented in this paper. Nevertheless, we believe that it is extremely important to consider the mathematical structure of the quantum conditions on a unified standing point. In this sense, the present paper complements the theories of Gutzwiller¹ and Littlejohn⁹.

Acknowledgment

This work was supported in part by the Grant in Aid from the Ministry of Education, Science, and Culture of Japan.

References

1. M.C. Gutzwiller, J. Math. Phys. *11*, 1791 (1970); *12*, 343 (1971).
2. R. Balian and C. Bloch, Ann. Phys. *60*, 401 (1970); *ibid.* *85*, 514 (1974).
3. (a) W.H. Miller, J. Chem. Phys. *56*, 38 (1972); (b) W.H. Miller, J. Chem. Phys. *63*, 996 (1975); (c) C. DeWitt-Morette, A. Maheshwari, and B. Nelson, Phys. Reports, *50*, 255 (1979); J.M. Robbins, to appear in Nonlinearity.
4. M.V. Berry and M. Tabor, Proc. Roy. Soc. (London) *A349*, 101 (1976); J. Phys. *A10*, 371 (1977).
See also, I.C. Percival, Adv. Chem. Phys. *36*, 1 (1977); A. Voros, Ann. Inst. Henri Poincaré, *24*, 31 (1976).
5. M.C. Gutzwiller, Phys. Rev. Lett. *45*, 150 (1980).
- 6.(a) M. Tabor, Physica *6D*, 195 (1983); M. Tabor, *Chaos and Integrability in Nonlinear Dynamics* (Wiley, New York, 1989); (b) D. Wintgen, Phys. Rev. Lett. *58*, 1589 (1987), *ibid.* *61*, 1803 (1988); (c) J.P. Keating and M.V. Berry, J.Phys. A, *L1139*, (1987).
7. C.P. Malta in Ref.8.
8. *The proceedings of the Adriatico Research Conference plus Miniworkshop on Quantum Chaos*. (Ed. H. Cerdeira, R.Ramaswamy, and M. Gutzwiller, World Scientific, Singapore, to appear in 1991).
9. R.G. Littlejohn, to appear in J. Math. Phys. and ref.8.
10. A preliminary report on the present work has been given in K. Takatsuka, in Ref.8.

11. K. Takatsuka, Phys. Rev. Lett. *61*, 503 (1988); Phys.Rev. *A39*, 5961 (1989).
12. A.J. Lichtenberg and M.A. Lieberman, *Regular and Stochastic Motion* (Springer, Berlin, 1983).
13. J.M. Greene, J. Math. Phys. *20*, 1183 (1979).
14. (a) E.J. Heller, Phys. Rev. Lett. *53*, 1515 (1984); E.J. Heller, in *Quantum Chaos and Statistical Nuclear Physics* (Ed. T.-H. Seligman and H. Nishioka, Springer, Berlin, 1986); (b) E.B. Bogomolony, Physica *D31*, 169 (1988); M.V. Berry, Proc. Roy. Soc. Lond. *A423*, 219 (1989).
15. (a) L.S. Schulman, *Techniques and Applications of Path Integration* (Wiley, New York, 1981); (b) V.P. Maslov and M.V. Fedoriuk, *Semiclassical Approximation in Quantum Mechanics* (Reidel, Dordrecht, 1981); (c) S. Levit and U. Smilansky, Ann. Phys. *108*, 165 (1977); S. Levit, K. Möhring, U. Smilansky, and T. Dreyfus, Ann. Phys. *114*, 223 (1978).
16. R.G. Littlejohn, Phys. Reports, *138*, 193 (1986); J.M. Robbins and R.G. Littlejohn, Phys. Rev. Lett. *58*, 1388 (1987); J.M. Robbins and R.G. Littlejohn, Phys. Rev. *A36*, 2953 (1987).
17. J.B. Keller, Ann. Phys. *4*, 180 (1958); J.B. Keller and S.I. Rubinow, Ann. Phys. *9*, 24 (1970).
18. A.M. Ozorio de Almeida, Nonlinearity *2*, 519 (1989).
19. M.V. Berry and K.E. Mount, Rep. Prog. Phys. *35*, 315 (1972).
20. P.M. Morse and H. Feshbach, *Methods of Theoretical Physics*. (McGraw-Hill, New York, 1953).
21. H. Goldstein, *Classical Mechanics*. (Addison-Wesley, Reading, 1980).
22. M.A. Mehta and N. De Leon, J. Chem. Phys. *89*, 882 (1988).
23. E.T. Whittaker, *A Treatise on the Analytical Dynamics of Particles and Rigid Bodies, 4th Ed.* (Cambridge Univ. Press, Cambridge, 1959).

24. See, for example, S.N. Rasband, *Chaotic Dynamics of Nonlinear Systems* (Wiley, New York, 1990).
25. M.V. Berry, Proc. Roy. Soc. Lond. *A400*, 229 (1985); *Nonlinearity 1*, 399 (1988), and ref.8.
26. A. Voros, J. Phys. A *21*, 685 (1988).
27. B. Eckhardt and E. Aurell, Europhys. Lett. *9*, 509 (1989).
28. K. Takatsuka, to be published.
29. (a) R. Bowen, Am. J. Math. *94*, 413 (1972); (b) V.M. Alekseev and M.V. Yakobson, Phys. Reports *75*, 287 (1981).
30. R.Z. Sagdeev, D.A. Usikov, and G.M. Zaslavsky, *Nonlinear Physics* (Harwood Academic Publishers, GmbH, 1988).

Table 1. The convention for choosing the roots from ib -plane

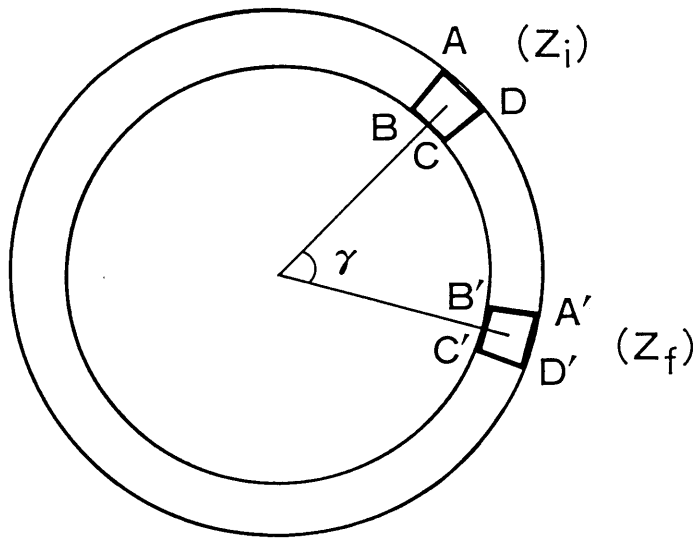
Name of Fixed Point	$t > 0$ a)	$t < 0$ b)
Elliptic	$i d $	$-i d $
Hyperbolic	$ c $	$ c $
Hyperbolic-with-reflection	$ c + i\pi$	$ c - i\pi$
General	$ c + i d $	$ c - i d $
	$ c - i d $	$ c + i d $

a) The roots to be taken for a positive time. b) The roots for a negative time.

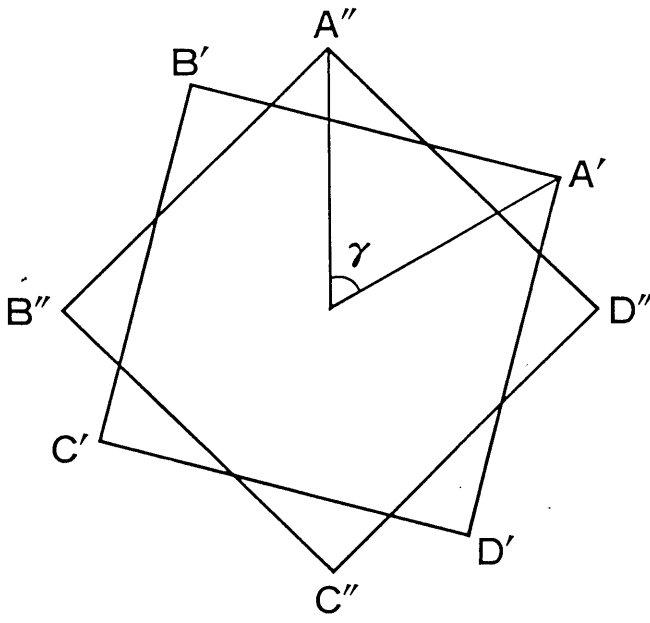
Figure Caption:

Fig.1

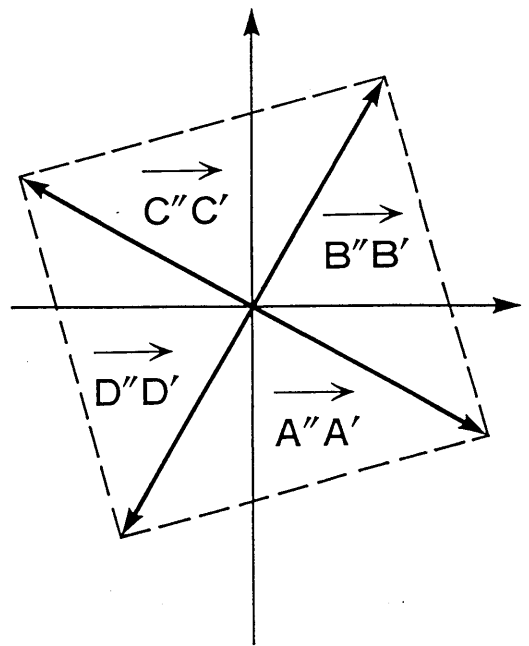
Geometrical meaning of $\partial(Z_f - Z_i)/\partial Z_i$ in a harmonic oscillator. (a) The motion of a volume element sandwiched by infinitesimally nearby orbits in a scaled phase space. (b) $\square ABCD$ is slidden to the position of $\square A'B'C'D'$ and denoted by $\square A''B''C''D''$. (c) A square formed by the vectors $\overrightarrow{A''A'}$, $\overrightarrow{B''B'}$, $\overrightarrow{C''C'}$, and $\overrightarrow{D''D'}$. The ratio of the area thus formed to that of $\square ABCD$ is equal to $\partial(Z_f - Z_i)/\partial Z_i = 4\sin^2(\gamma/2)$.



(a)



(b)



(c)

Extraction of Accurate Frequencies from the Fast-Fourier-Transform Spectra

Kazuo Takatsuka

Department of Chemistry, College of General Education

Nagoya University

Nagoya 464-01, Japan

Abstract

The Fast Fourier Transformation (FFT) is well-known to be extremely fast and useful. However, its spectrum is quite often not accurate, because it is a discrete transformation and, further, the effect of finite range of sampling, the so-called Gibbs phenomenon, produces long tails. Here a very simple and efficient method to extract the accurate frequencies and the amplitudes of discrete spectra from FFT data is proposed. No window function is used in the present method. The resultant frequencies have been found to be extremely accurate.

I. INTRODUCTION

Quasi-periodic functions which are of the following form

$$\phi(t) = \sum_{m \geq 0} C_m \cos(f_m t) + S_m \sin(f_m t) \quad (-\infty \leq t \leq \infty) \quad (1-1)$$

appear frequently in science and engineering. For example, in classical mechanics, coordinates and momenta of a particle in multiply periodic motions, such as molecular vibrations, can be represented as in the above expression.[1] Theoretically, the action-angle variables can be obtained by a certain procedure[2], in which the frequencies (f_m) and amplitudes (S_m and C_m), play essential roles. The continuous Fourier transformation can provide these values in principle. In practice, however, it is quite often required to extract them from a finite set of discrete sampling points with high accuracy and high speed. From the view point of speed, the celebrated Fast Fourier Transformation (FFT) technique is almost exclusively used practically. However, the accuracy of the results by FFT is considerably limited, since FFT is not really a continuous integral transformation but a discrete one performed within a finite range. Therefore, if an actual frequency, say f_m , is located in between two frequencies which are given by FFT automatically, the FFT spectra at these sandwiching points oscillate violently with different signs. Furthermore, these peaks have long tails, which is due to sudden truncation of the series of sampling data (the so-called Gibbs phenomenon). An example of this situation is depicted in Fig.1.

One of the methods to avoid the long-tail behavior is to apply the so-called window technique. It is well-known that a bell-shaped window function, for instance, can well reduce the truncation effect.[3] On the other hand, the data thus windowed are biased and the height of the spectral peaks is lowered. In order to suppress the tails and also to obtain accurate heights simultaneously, FFT is sometimes performed two times with

different type of windows for each purpose. A recent and important example of the application of a window technique can be found in ref.[2], which also briefly reviews the former works. It is also a usual practice to vary the length of sampling set to lead one of the FFT frequencies to come very close to a true frequency. These procedures are generally very tedious.

In this paper, I propose a method to obtain the accurate frequencies and amplitudes of quasi-periodic functions from their FFT spectra with no use of such a window function technique. The idea is very simple and its implementation and usage are extremely easy.

II. BASIC PROCEDURES

A. FFT

We consider a function having only two frequencies in Eq.(1-1) without loss of generality for the presentation of our procedure, namely,

$$\phi(t) = \phi_f(t) + \phi_g(t) \quad (2-1a)$$

with

$$\phi_f(t) = C_f \cos(ft) + S_f \sin(ft) \quad (2-1b)$$

and

$$\phi_g(t) = C_g \cos(gt) + S_g \sin(gt). \quad (2-1c)$$

The frequencies f and g are assumed not very close to each other throughout the present paper. The cosine-FFT and sine-FFT are usually defined as

$$F_c(k) = \frac{2}{N} \sum_{j=0}^{N-1} \cos\left(\frac{2\pi kj}{N}\right) \{\phi_f(j\Delta t) + \phi_g(j\Delta t)\} \quad (2-2)$$

and

$$F_s(k) = \frac{2}{N} \sum_{j=0}^{N-1} \sin\left(\frac{2\pi kj}{N}\right) \{\phi_f(j\Delta t) + \phi_g(j\Delta t)\} \quad (2-3)$$

with

$$\Delta t = \frac{T}{N}, \quad (2-4)$$

where T and N are the sampling length and number, respectively.

By inserting Eqs.(2-1) to Eqs.(2-2) and (2-3), we have

$$F_c(k) = A_{cc}(k, f)C_f + A_{cs}(k, f)S_f + A_{cc}(k, g)C_g + A_{cs}(k, g)S_g \quad (2-5)$$

and

$$F_s(k) = A_{sc}(k, f)C_f + A_{ss}(k, f)S_f + A_{sc}(k, g)C_g + A_{ss}(k, g)S_g. \quad (2-6)$$

The definitions of the above functions such as $A_{sc}(k, f)$ are obvious. For example,

$$A_{cs}(f, k) = \frac{2}{N} \sum_{j=0}^{N-1} \cos\left(\frac{2\pi kj}{N}\right) \sin(fj\Delta t). \quad (2-7)$$

It is clear that if f and g are known, Eqs.(2-5) and (2-6) can be viewed as simultaneous equations to determine the amplitude factors C_f , S_f , C_g , and S_g with appropriate choice of k .

B. Approximate Evaluation of FFT

Let us rewrite Eq.(2-2) as follows,

$$F_c(k) = \frac{2}{T} \sum_{j=0}^{N-1} \cos\left(\frac{2\pi kj}{T} \Delta t\right) \{\phi_f(fj\Delta t) + \phi_g(fj\Delta t)\} \Delta t. \quad (2-8)$$

Under a condition that Δt is "sufficiently" small, the above sum is evaluated approximately by an integral

$$F_c(k) \cong \frac{2}{T} \int_0^T dt \cos\left(\frac{2\pi kt}{T}\right) \{ \phi_f(ft) + \phi_g(gt) \}, \quad (2-9)$$

which is simply a return to the continuous Fourier transform. This integral can be evaluated exactly, the result being

$$\begin{aligned} F_c(k) = & \frac{C_f}{T} \frac{\sin(fT)}{f - \frac{2\pi k}{T}} + \frac{C_f}{T} \frac{\sin(fT)}{f + \frac{2\pi k}{T}} - \frac{S_f}{T} \frac{\cos(fT) - 1}{f - \frac{2\pi k}{T}} - \frac{S_f}{T} \frac{\cos(fT) - 1}{f + \frac{2\pi k}{T}} \\ & + \frac{C_g}{T} \frac{\sin(gT)}{g - \frac{2\pi k}{T}} + \frac{C_g}{T} \frac{\sin(gT)}{g + \frac{2\pi k}{T}} - \frac{S_g}{T} \frac{\cos(gT) - 1}{g - \frac{2\pi k}{T}} - \frac{S_g}{T} \frac{\cos(gT) - 1}{g + \frac{2\pi k}{T}} \end{aligned} \quad (2-10)$$

In the similar way, sine-FFT is also evaluated as

$$\begin{aligned} F_s(k) = & \frac{C_f}{T} \frac{\cos(fT) - 1}{f - \frac{2\pi k}{T}} - \frac{C_f}{T} \frac{\cos(fT) - 1}{f + \frac{2\pi k}{T}} + \frac{S_f}{T} \frac{\sin(fT)}{f - \frac{2\pi k}{T}} - \frac{S_f}{T} \frac{\sin(fT)}{f + \frac{2\pi k}{T}} \\ & + \frac{C_g}{T} \frac{\cos(gT) - 1}{g - \frac{2\pi k}{T}} - \frac{C_g}{T} \frac{\cos(gT) - 1}{g + \frac{2\pi k}{T}} + \frac{S_g}{T} \frac{\sin(gT)}{g - \frac{2\pi k}{T}} - \frac{S_g}{T} \frac{\sin(gT)}{g + \frac{2\pi k}{T}} \end{aligned} \quad (2-11)$$

In Eqs.(2-10) and (2-11), the oscillatory behavior shown in Fig.1 is quite apparent. Before proceeding, let us confirm that in these expressions f , g , C_f , and S_f are unknown, while $F_c(k)$ and $F_s(k)$ are known as the FFT spectra.

C. First Guess of the Frequencies

We assume that the true frequency f happens to be located in the range

$$\frac{2\pi}{T} K < f < \frac{2\pi}{T} (K+1) \quad (2-12)$$

for a given K , which can be inspected directly in the FFT spectra or in its power. Then the far dominant term in Eq.(2-10) for $k=K$ is

$$F_c(K) \approx \frac{C_f}{T} \frac{\sin(fT)}{f - \frac{2\pi K}{T}} \quad (2-13)$$

and that for $k=K+1$,

$$F_c(K+1) \approx \frac{C_f}{T} \frac{\sin(fT)}{f - \frac{2\pi(K+1)}{T}} \quad (2-14)$$

The other terms are very small unless both f and k are close to zero. In addition, we have assumed that T is chosen so that $\sin(fT)$ is not very small.

Now f can be guessed with use of the ratio defined by

$$X_c = \frac{F_c(K+1)}{F_c(K)} \quad (2-15)$$

such that

$$f \approx \frac{2\pi K}{T} - \frac{2\pi}{T} \frac{X_c}{1-X_c} \quad (2-16)$$

Thus we can make a first guess of f . The similar procedure can be carried out using the sine-FFT data. We have observed that the difference between the two guesses is generally very small and accordingly we adopt the simple average of them hereafter. Moreover, our numerical experience has shown that the f value thus guessed is already fairly close to the exact one. The same procedure can be carried out independently for the frequency g .

D. First Guess of the Amplitudes (Linear Equation Method)

Now that we have the first guess of f and g , Eqs.(2-5) and (2-6) can be made use of to obtain the amplitudes. It is assumed that g satisfies

$$\frac{2\pi}{T} L < g < \frac{2\pi}{T} (L + 1) . \quad (2-17)$$

Further let K' be either one of K and $K+1$, which is closer to f in the sense of Eq.(2-12), and similarly choose L' in Eq.(2-17). Then by putting $k=K'$ and $k=L'$ in Eqs.(2-5) and (2-6), we have simultaneous linear equations, the number of which is equal to that of the unknown. In our example, that is

$$\begin{bmatrix} A_{cc}(K', f) & A_{cs}(K', f) & A_{cc}(K', g) & A_{cs}(K', g) \\ A_{sc}(K', f) & A_{ss}(K', f) & A_{sc}(K', g) & A_{ss}(K', g) \\ A_{cc}(L', f) & A_{cs}(L', f) & A_{cc}(L', g) & A_{cs}(L', g) \\ A_{sc}(L', f) & A_{ss}(L', f) & A_{sc}(L', g) & A_{ss}(L', g) \end{bmatrix} \begin{bmatrix} C_f \\ S_f \\ C_g \\ S_g \end{bmatrix} = \begin{bmatrix} F_c(K') \\ F_s(K') \\ F_c(L') \\ F_s(L') \end{bmatrix} \quad (2-18)$$

Thus the first guess of the amplitudes can be obtained. The matrix elements in Eq.(2-18) can be evaluated through the expressions as in Eq.(2-7). Alternatively, they can be approximated by the integral representation as in Eq.(2-9). For example, the approximation of $A_{cs}(f, K)$ is obtained as a coefficient of C_f in Eq.(2-10) by comparing Eqs.(2-5) and (2-10). From this approximation, it is seen that if fT and/or gT are very close to an integer multiple of 2π and k is not properly chosen, the matrix $\{A_{sc}\}$ becomes nearly singular. This was already pointed out below Eq.(2-14).

The above method based on Eq.(2-18) is convenient in that the matrix $\{A_{sc}\}$ and the vector $\{F_c\}$ are decoupled more or less to each frequency region as the functions of k . For example, the off-diagonal terms $A_{sc}(K', g)$'s in Eq.(2-18) are all small if f and g are sufficient separated. This fact will lead to an iterative method to solve Eq.(2-

18) locally at each frequency part as will be described in subsection F. A major drawback of solving Eq.(2-18) is, however, that the evaluation of $\{A_{SC}\}$ is a little time consuming and moreover certain error is expected to arise. Remember that f and g to be put in $\{A_{SC}\}$ are approximate ones, which were obtained in the preceding subsection. Even if both f and g are reasonably good, $\sin(ft)$ and $\cos(ft)$, for example, deviate from the exact values as t becomes large and correspondingly this takes place as j gets large in Eq.(2-7). A very simple way to circumvent this is to use the initial data $\{\phi(j\Delta t) | j = 1, 2, \dots, N\}$ directly. We have equations

$$\cos(fj\Delta t)C_f + \sin(fj\Delta t)S_g + \cos(gj\Delta t)C_g + \sin(gj\Delta t)S_g = \phi(j\Delta t) \quad (2-19)$$

for $j = 0, 1, \dots, N-1$. Here again f and g are only approximated quantities. Equations (2-19) can be inverted to obtain the amplitudes, where j 's have to be chosen to be small enough, and the resultant linear equations should be made mutually independent.

E. Decoupling of the tail effects (Improvement of the frequencies)

We have now the first estimate of amplitudes, which can in turn be made use of in order to improve the first guess of the frequencies. We remember that the frequencies have been estimated through Eqs.(2-15) and (2-16), in which the original (raw) spectral data of FFT were adopted. However, each peak in FFT spectrum is contaminated by long tails extended from the other peaks. Let us look at the FFT spectrum at $F_c(K)$, that is

$$F_c(K) \approx \frac{C_f}{T} \frac{\sin(fT)}{f - \frac{2\pi K}{T}} + \frac{2}{N} \sum_{j=0}^{N-1} \cos\left(\frac{2\pi Kj}{N}\right) \{C_g \cos(gj\Delta t) + S_g \sin(gj\Delta t)\} \quad (2-20)$$

The second term in the right hand side forms the tail from the peak at the frequency g .

The magnitude of the tail is not necessarily small in general, since it looks like

$$\frac{C_g}{T} \frac{\sin(gT)}{g - \frac{2\pi K}{T}} + \frac{C_g}{T} \frac{\sin(gT)}{g + \frac{2\pi K}{T}} - \frac{S_g}{T} \frac{\cos(gT) - 1}{g - \frac{2\pi K}{T}} - \frac{S_g}{T} \frac{\cos(gT) - 1}{g + \frac{2\pi K}{T}} \quad (2-21)$$

and thus its range is very long, just like the Coulomb potential. It is a trivial work to remove the effect of the tail in Eq.(2-20) and thus we obtain the purer spectrum, for instance,

$$F'_c(K) = F_c(K) - \frac{2}{N} \sum_{j=0}^{N-1} \cos\left(\frac{2\pi Kj}{N}\right) \{C_g \cos(gj\Delta t) + S_g \sin(gj\Delta t)\} \quad (2-22)$$

which should be brought back to Eq.(2-15) to refine the frequencies.

The renewed frequencies are again inserted into Eq.(2-18) or Eq.(2-19) to improve the amplitudes. This entire process should be iterated until a convergence is attained.

F. The Iteration Method for the Amplitudes

When we treat a spectrum composed of many peaks, the matrices and vectors in Eq.(2-18) become large. To avoid this, we can solve Eq.(2-18) in an iterative manner: Going back to Eqs.(2-10) and (2-11), we can set up the following linear equations for the amplitudes associated with the frequency f ;

$$\begin{aligned}
& \begin{bmatrix} \frac{\sin(fT)}{fT-2\pi K} + \frac{\sin(fT)}{fT+2\pi K} & -\frac{\cos(fT)-1}{fT-2\pi K} - \frac{\cos(fT)-1}{fT+2\pi K} \\ \frac{\cos(fT)-1}{fT-2\pi K} - \frac{\cos(fT)-1}{fT+2\pi K} & \frac{\sin(fT)}{fT-2\pi K} - \frac{\sin(fT)}{fT+2\pi K} \end{bmatrix} \begin{bmatrix} C_f \\ S_f \end{bmatrix} \\
& = \begin{bmatrix} F'_c(K) \\ F'_s(K) \end{bmatrix}
\end{aligned} \tag{2-23}$$

where F' is the spectrum in which the tail effect have been subtracted as in Eq.(2-22). The similar set of equations can be set up for each frequency. In the calculation of the purified spectra F' , however, the amplitudes should have been known beforehand. Thus the procedure should be carried out iteratively.

III. NUMERICAL EXAMPLES

Some simple, but not necessarily easy, examples are presented here to show how the method works. Our presentation is confined to only two frequency cases for the sake of simplicity, although our procedure and program are general. The iteration procedure from subsection A to E has been performed. The matrix $\{A_{SC}\}$ has been evaluated directly with Eq.(2-7).

Our sample functions are chosen to be exactly the same form as in Eq.(2-1). One is

$$\phi_1 = \cos(5.5t) + 2.0 \sin(11.0t)$$

where two frequencies are far apart and the other is

$$\phi_2 = \cos(10.5t) + 2.0 \sin(11.0t)$$

which has relatively close frequencies, in which the tails have stronger magnitude.

Δt , T , and N are varied. The standard values of Δt here is 0.1, which is not very small compared with the shortest period in the above trigonometric functions involved,

that is about 0.571. The standard value of N here is 2048 (2¹¹). This is a small scale FFT. In short, our examples are set so that the conditions are not exceptionally good, or rather relatively worse than the usual applications of FFT. The resolution of a frequency in FFT is

$$\Delta f = \frac{2\pi}{T} = \frac{2\pi}{N \Delta t} \quad (2-24)$$

For our standard values of Δt and N , Δf is about 0.030680, which means the resolution of a frequency by the present FFT is up to the first decimal point below zero.

The reach to a convergence has been judged when the successive improvement of the frequencies gets within 10⁻¹³. The number of iterations was generally about 5 to 10. Since the first guess of the frequencies and amplitudes are not *relatively* good, the second iteration improves their values significantly. The convergence after the second iteration is hence slow.

The results are shown in Table 1. The method A is referred to a procedure using Eq.(2-18), and B is to that based on Eq.(2-19). As seen in the table, the results obtained are generally very good. In particular, the accuracy of the frequencies is far beyond the FFT resolution mentioned above.

On the other hand, the accuracy of the amplitude is not as good as that of the frequencies. In particular, the method A reproduces the amplitudes rather poorly as noted in subsection D. The method B, which is faster, gives better results as anticipated.

In Eq.(2-9), the sum has been approximated by an integral. This must be crucial. Hence the result depends on how small Δt can be chosen. On the other hand, if we let Δt become smaller with keeping N constant, Δf becomes larger in accordance with Eq.(2-24), which in turn means that the dominance by the single term in Eq.(2-13) is deteriorated. Thus the better results are expected only when N is increased

simultaneously. We choose $\Delta t = 0.05$ and $N = 4096 = 2^{12}$. As seen in Table 1, the errors both in the frequencies and amplitudes have been reduced by the factor about 2.

IV. CONCLUDING REMARKS

We have proposed an efficient and simple idea to extract the frequencies and amplitudes of a quasi-periodic function from FFT spectra. The results have been found very accurate. One of the most annoying parts of the numerical procedure of FFT is the selection of window functions. It is hoped that the present method can relax this situation in part.

Since the purpose of the present paper is to present the outline of the basic idea, the sophistication of the procedure has not been mentioned at all. For example, the acceleration of the iteration process can be achieved by an extrapolation method or its analogue.

Finally, the present procedure has been worked out in a study of onset of Hamilton chaos. Its theoretical aspect and numerical examples will be presented elsewhere.[4]

Acknowledgment

This work was supported in part by the Grant in Aid from the Ministry of Education, Science, and Culture of Japan.

References

1. H. Goldstein, *Classical Mechanics*, 2nd ed. (Addison-Wesley, Reading, 1980).
2. C.C. Martens and G.S. Ezra, *J. Chem. Phys.* **83**, 2990 (1985); *ibid.* **86**, 279 (1986).
3. a) O. Brigham, *The Fast Fourier Transform* (Prentice Hall, New Jersey, 1974).
b) M. Hino, *Spectral Analysis* (Asakura, Tokyo, 1977). This is an excellent book, but, unfortunately, available only in Japanese.
4. K. Takatsuka, to be published.

Table 1. The frequencies and amplitudes extracted from the FFT spectra

Methods ^a	f	C_f	S_f	g	C_g	S_g
ϕ_1						
Exact	5.500000	1.000000	0.000000	11.000000	0.000000	2.000000
A^b	5.500069	0.990846	0.006965	11.000004	-0.000806	1.999547
A^c	5.500035	0.995401	0.003507	11.000002	-0.000400	1.999776
B^b	5.500069	1.000005	0.000018	11.000006	-0.000005	1.999991
B^c	5.500034	1.000002	0.000010	11.000003	-0.000002	1.999995
ϕ_2						
Exact	10.500000	1.000000	0.000000	11.000000	0.000000	2.000000
A^b	10.500061	0.990914	0.006258	11.000001	-0.000243	1.999885
A^c	10.500030	0.995432	0.003152	11.000001	-0.000103	1.999953
B^b	10.500055	1.000108	0.000072	11.000016	-0.000107	1.999928
B^c	10.500027	1.000057	0.000032	11.000008	-0.000057	1.999968

a) Method A is based on Eq.(2-18), while B on Eq.(2-19).

b) $\Delta t = 0.1$, $N=2^{11}$ c) $\Delta t = 0.1$, $N=2^{12}$

Figure Caption:

The cosine-FFT spectrum for $\phi(t) = \cos(10.0t) + 2.0 \sin(11.0t)$: One of the discretized frequencies given by FFT happens to be extremely close to 10.0, and correspondingly a single sharp peak is produced. On the other hand, the sine component in $\phi(t)$ is detected even in the cosine transformation with a large amplitude oscillation, which is accompanied by long tails.

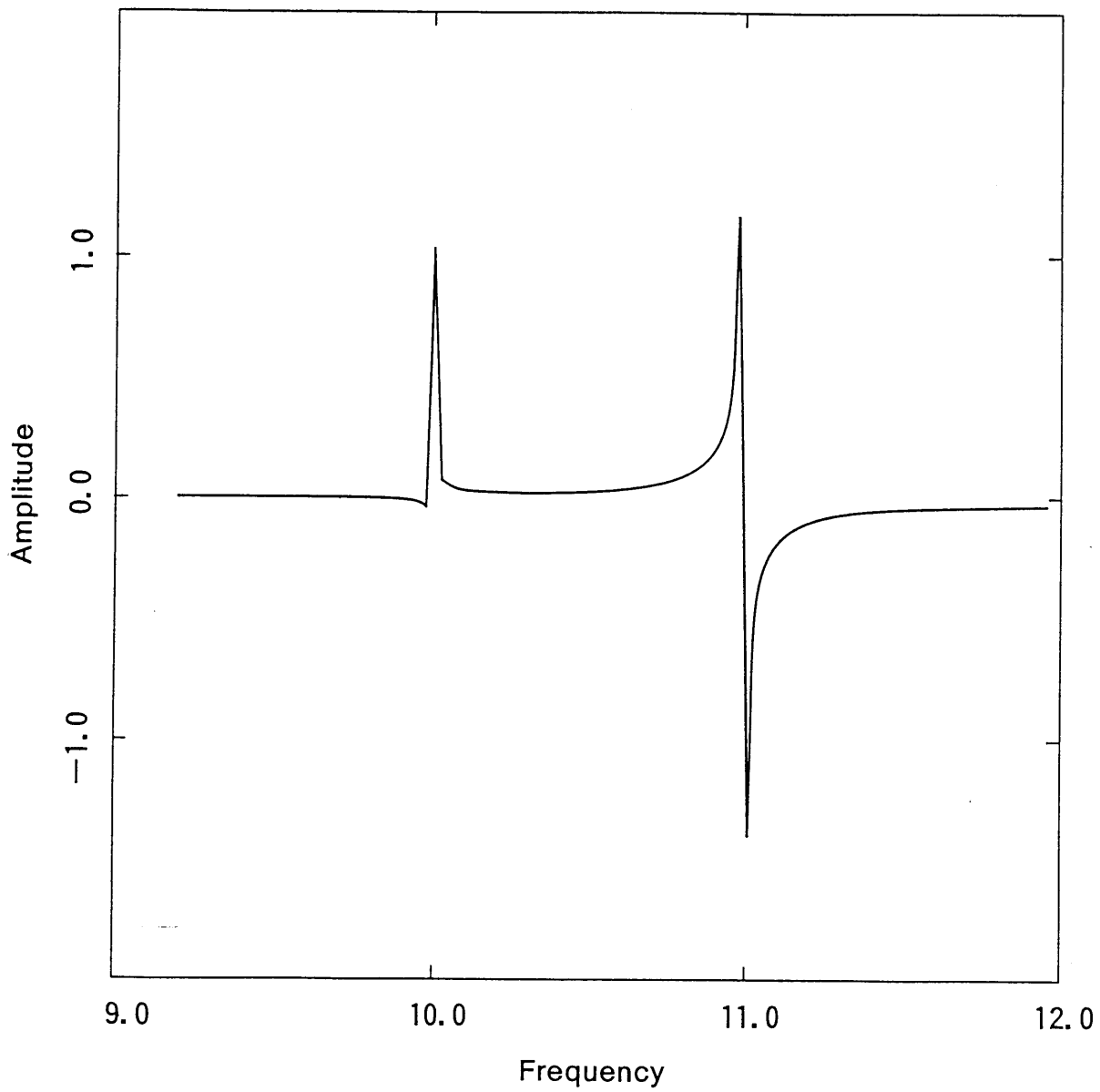


Fig. 1

Possible Onset of Entrainment in Hamilton Chaos

Kazuo Takatsuka

Department of Chemistry, College of General Education

Nagoya University

Nagoya 464-01, Japan

Abstract

A break-up of an invariant torus is monitored in terms of the spectrum of the quasi-action variable which is newly defined as a continuous function of frequency. We have found a new characteristic phenomenon called "entrainment" at the onset of chaos, in which two discrete peaks in a regular regime merge into a continuous spectrum as a system steps into chaos and the resultant band has significant magnitude only in between the original frequencies.

I. INTRODUCTION

Chaos has been one of central subjects in recent advances of various studies on dynamical systems¹. Systematic analyses on the mechanism of chaos have been made with the Poincaré surface of section, which gives a global structure of phase flow¹. On the other hand, chemists are often interested in the characteristic behavior of an each trajectory of relatively large molecules and liquid-state systems, and the surface of section is too limited for this purpose. In quantum chaos, the density of states² and the so-called quantum scars³ are characterized in terms of periodic orbits², which also means that the analysis of each trajectory is unavoidable.

Here we consider only Hamilton chaos¹, which is simply defined by the break of an invariant torus. As is well known, the "size" of an invariant torus is measured by the action variables, which are the constants of motion of a system. A natural question here is whether a classical trajectory we happen to have at hand is on a torus or not. If yes, how large are the action variables? These values can be directly made use of for the semiclassical determination of quantum levels based on the EBK conditions⁴. In case of chaos, on the other hand, what happens to the action variables, particularly at the onset?

Recently we have devised a practical method to calculate action variables and their frequencies⁵, which is based on a geometrical consideration in phase space. A natural generalization of the action variable, which we call the quasi-action variable, have also been studied to investigate the transition from regular to chaotic motions. The quasi-action variable is defined as a function of frequency. In our numerical study of chaos, we have observed various patterns in the spectra of the quasi-action. The rest of the present paper is devoted to reporting a particularly characteristic feature of the onset of chaos, which we want to call "entrainment" mechanism.

We first review very briefly the definition of the quasi-action variable⁵. Let us assume a case where a system has a set of action variables. Suppose we have a classical trajectory in $2N$ dimensional phase space as depicted in Fig.1. Let $\vec{Z}(t) = \{ \vec{Z}_i(t) \} = \{ q_i(t), p_i(t) \}$ ($i=1,2,\dots,N$) be a phase space point on the trajectory, where $q_i(t)$ and $p_i(t)$ are the coordinates of the position and its conjugate momenta, respectively, at time t . The suffix i is reserved for general canonical coordinates. We define the following oriented area;

$$B(t) = \frac{1}{2} \sum_{k=0}^{M-1} \sum_{i=1}^N \vec{Z}_i(t_k) \wedge \vec{Z}_i(t_k + \Delta t) - \frac{1}{2} \sum_{i=1}^N \vec{Z}_i(0) \wedge \vec{Z}_i(t), \quad (1)$$

where $t_0=0$, $t_k=k\Delta t$, and $M=t/\Delta t$. The limit $\Delta t \rightarrow 0$ should be taken. The geometrical meaning of $B(t)$ is the sum of the segment areas in Fig.1 (the shaded area), each of which is formed by the projection of the trajectory onto, say, Z_i -plane and that of a straight line connecting $Z(0)$ and $Z(t)$. By the definition of $B(t)$, it is canonically invariant⁶.

For a one-dimensional oscillator, it is quite obvious that $B(t)$ becomes equivalent to the action variable $I = \oint p dq$ at $t = T$, where T is the period ($= 2\pi/\omega$). In a multi-dimensional case, the situation is not so simple. However, the canonical invariance allows to transform $B(t)$ to the action-angle phase space ($I_k-\theta_k$ space) invariantly. [The suffix k is used for the action-angle variables.] In Fig.2, the shaded area (segment), denoted by $B_k(t)$, corresponds to the projected area onto $I_k-\theta_k$ plane, where the trajectory is represented by the straight line, while the straight line of $Z(0)Z(t)$ in the original coordinates (see Fig.1) is transformed into a curved line. The sum of all $B_k(t)$'s is $B(t)$. As in the one-dimensional case, $B_k(t)$ coincides with the action variable I_k at $t = T_k$, where T_k is the period in the k -th angle coordinate (mod. 2π).

Since $B_k(t)$ is a periodically increasing function with a linear term of t and an oscillating part whose period is $T_k (= 2\pi/\omega_k)$

$$B_k(t) = a^k t + \sum_{m=0}^{\infty} [b_m^k \sin(m\omega_k t) + c_m^k \cos(m\omega_k t)], \quad (2)$$

where the coefficients a , b 's, and c 's are all constant. Judging from this expansion, the time derivative of $B_k(t)$ must be more feasible for the Fourier analysis. It is written as

$$\begin{aligned} B_k'(t) &= a^k + \omega_k \sum_{m=0}^{\infty} m [b_m^k \cos(m\omega_k t) - c_m^k \sin(m\omega_k t)] \\ &\equiv a^k + F_k(t) \end{aligned} \quad (3)$$

where the second equality defines the function $F_k(t)$, and $B'(t) = \sum B_k'(t)$. Thus the Fourier transform of $B'(t)$ should provide the frequencies corresponding to the angle variables. Furthermore, the action variables can also be deduced from the Fourier data as

$$I_k = 2\pi a_k = -2\pi \sum_{m=0}^{\infty} m b_m^k. \quad (4)$$

This has been derived under the following conditions $B_k(0) = 0$, $B_k'(0) = 0$, and $B_k'(T_k) = I_k$.

Incidentally, it is noteworthy that the expansion of $B'(t)$ does not have the combination bands of different modes. This is in a marked contrast to the Fourier expansion of primitive quantities⁷ such as $q_i(t)$, since we have

$$q_i(t) = \sum_{j_1}^{\infty} \cdots \sum_{j_N}^{\infty} D_{j_1 j_2 \cdots j_N}^i \exp[i(j_1 \omega_1 + j_2 \omega_2 + \cdots + j_N \omega_N)t]. \quad (5)$$

In practice, the perfect form of the Fourier expansion of $B'(t)$ is not always realized because of numerical errors mainly due to the finite time difference approximation to the

various differential equations. Since $B'(t)$ is expected to increase monotonically as t , or $B_k'(t) \geq 0$, we can determine I_k variationally as

$$I_k = - \frac{2\pi}{\omega_k} F_k(t_{min}), \quad (6)$$

where t_{min} is a t which makes $F_k(t)$ minimum. t_{min} is actually very close to 0, which indicates that the condition $B_k'(0)=0$ used to derive Eq.(4) is almost satisfied. A practical method to calculate $B'(t)$ will be reported elsewhere.⁵

We next try to extend the above procedure to define the quasi-action variable. We first note that $-F_k(t_{min})$ is essentially equivalent to the square root of the power spectrum of $F_k(t_{min})$,

$$P_k = \sum_{m=1} P_k^m(m\omega_k) = \sum_{m=1} (\omega_k m)^2 [(b_m^k)^2 + (c_m^k)^2] \quad (7)$$

Generally the contributions to P_k from the second harmonics ($m=2$) and the higher ones are very small as compared to the fundamental component, and hence, we have (see Eq.(6))

$$I_k \approx \frac{2\pi}{\omega_k} [P_k^1(\omega_k)]^{1/2}, \quad (8)$$

On the other hand, $B'(t)$ can be computed equally well for a chaotic trajectory. Since the Fourier expansion and the decomposition into the k -th action-angle component as in Eq.(3) are both meaningless, and since the concept of the overtone of discrete spectrum loses the sense as well, we simply define the total power spectrum of $B'(t)$, after the constant term is subtracted. This is denoted by $P(\omega)$. Then in the analogy of Eq.(8) we define the quasi-action variable as

$$\tilde{I}(\omega) \equiv \frac{2\pi}{\omega} [P(\omega)]^{1/2}, \quad (9)$$

which is a continuous function of ω . In an integrable system, the quasi-action variable has a discrete spectrum at frequencies of $m\omega_k$ ($k=1,\dots,N$; $m=1,2,\dots$) [see Fig.3(a)]. As stated above, the components due to $m=2$ and the higher ones are very small in general. The quasi-action variables at the fundamental frequencies are the same as I_k of Eq.(8), and thus gives a very good approximation to the true action variables. In a chaotic system, on the other hand, the quasi-action variable in Eq.(9) provides a continuous spectrum, the height of which is a function of the time length of running a classical trajectory. The longer is the running time, the lower becomes the peak height of the quasi-action variable. This is not the case in an integrable case, since there is no constant of motion except for the total energy in chaos.

We now present a very characteristic feature of chaos monitored by the quasi-action variable. The system of our application is the Henon-Heiles Hamiltonian $H = \frac{p_x^2}{2m_x} + \frac{p_y^2}{2m_y} + \frac{1}{2}(x^2 + y^2 + 2x^2y - \frac{2}{3}y^3)$ with a choice of $m_x = 1.0$ and $m_y = 1.5$, which breaks the symmetry. A pattern of the so-called intermittency or burst gives rise to in the standard choice, $m_x = m_y = 1.0$, which is discussed elsewhere⁵. We have carried out a series of computations with changing the total energy E around the onset point of chaos up to the dissociation limit. The initial conditions of the trajectories are chosen so that $x = y = 0.0$ with their associated momenta being positive and the fraction of the energy assigned to the x -coordinate is 40%.

In Fig.3, the quasi-action variables with some energies are displayed. In case of $E = 0.1$ (the panel (a)), the two strong discrete peaks directly indicate that the trajectory is running on a torus with those fundamental frequencies and approximate action variables. All

the small peaks in this panel are the noise mainly due to the FFT (Fast-Fourier-Transform), and they are actually almost invisible in the power spectrum in Eq.(9). The overtone components, which are very small, are not displayed. Also, the small frequency part is omitted here, which should bear a direct relation to the $1/f$ noise (see.Eq.(9)).

In the panel (b) of Fig.3 ($E=0.105$), a continuous spectrum indicating the onset of chaos is observed, although the true onset energy for our initial conditions is a little lower than $E=0.105$. The cases of $E=0.10583$ and $E=0.1075$, the panels (c) and (d) in Fig.3, respectively, have even stronger continuous spectra. The occurrence of the continuous spectra in chaos has been pointed out by the other authors⁸ already, who have confirmed the break down of the expansion in Eq.(5). What is important in our findings common in the panels (a) to (e) is that the continuous spectra have significant intensity only in between the original fundamental frequencies. (By the way, the higher components around the second harmonics have very small magnitudes.) This very characteristic feature continues at least up to $E=0.125$ with slight shift of the positions. And further up in $E=0.145$, the panel (f) in Fig.3, more violent chaos takes place to break this characteristic feature. However, we can still observe the significant trace of the two strong peaks. This trace of the peaks of regular regime cannot be seen explicitly in Poincaré section. It should be mentioned that the running time of the classical trajectories do not alter the features.

Qualitatively, the above characteristic phenomenon indicates that the two "independent" (in the sense of the two independent actions) vibrational modes tend to synchronize to each other, after the restriction that the torus should exist is removed. It is well-known in mechanical vibration that when a perturbation having a constant frequency is applied to a vibrator with a different frequency, the latter frequency can be absorbed (pulled) into the same one as the outer frequency under a certain condition. This phenomenon, first found by Huygens, is called entrainment⁹. In this sense, the onset of the present chaos looks similar to the entrainment. Two major differences should be noted between the simple

entrainment and our onset of chaos: First, our system is not dissipative but conservative, which means that it cannot have a sink or limit cycle to which the system is absorbed with fixed frequencies. On the contrary, Poincaré's recurrence theorem requires that a motion should come back to an area very close to the original point in phase space. Thus the "instantaneous" frequency pulled to one direction has to be pushed back eventually. Second, although one of the vibrational modes in our system can be viewed as an outer perturbation applied to the other, the analogy to the entrainment is far from completeness, since both modes changes their frequencies from time to time because of high nonlinearity.

In spite of the differences mentioned above, we would like to call the present onset "entrainment", since synchronization (pulling each other) of the frequencies are very impressive. This view can be complemented by the Poincaré surface of section. In Figs.4(a) and 4(b), we have the surfaces of section due to the trajectory of $E=0.1$, which are taken at $x = 0$ and $y = 0$, respectively. Similarly, Figs.4(A) and 4(B) display those for $E=0.105$. Comparing Figs.4(a) and 4A shows that the manifold occupied by the trajectory is inflated outward as E has changed from 0.1 to 0.105. On the other hand, Figs.4(b) and 4(B) indicate that the "diameter" of this direction has shrunk inward. This does not necessarily provide the direct evidence of the entrainment, since the size of the manifolds are not always related to the frequency. However, generally speaking, the outer manifold tends to have the smaller frequency. Thus the entrainment mechanism seems consistent with the Poincaré surfaces.

We have reported a very characteristic phenomenon in the onset of Hamilton chaos based on the numerical experiment with the quasi-action variable. The "entrainment" can be one of the general mechanisms of mode mixing in chaos, and can provide a relationship between the dynamics of open and closed systems.

ACKNOWLEDGMENT

This work was supported in part by the Grant in Aid from the Ministry of Education, Science, and Culture of Japan.

REFERENCES

1. A.J. Lichtenberg and M.A. Lieberman, *Regular and Stochastic Motion* (Springer, Berlin, 1983); R.Z. Sagdeev, D.A. Usikov, and G.M. Zaslavsky, *Nonlinear Physics*. (Harwood Academic Publishers, GmbH, 1988).
2. M.C. Gutzwiller, *J. Math. Phys.* *11*, 1791 (1970); *12*, 343 (1971).
3. E.J. Heller, *Phys. Rev. Lett.* *53*, 1515 (1984); E.B. Bogomolny, *Physica D31*, 169 (1988); M.V. Berry, *Proc. R. Soc. Lond.* *A423*, 219 (1989).
4. C.C. Martens and G.S. Ezra, *J. Chem. Phys.* *83*, 2990 (1985); *ibid.* *86*, 279 (1986); S. Sinha and R. Ramaswamy, *Mol. Phys.* *67*, 335 (1989).
5. K. Takatsuka, to be published.
6. V.I. Arnold, *Mathematical Methods of Classical Mechanics*. (Springer, Berlin, 1978).
7. H. Goldstein, *Classical Mechanics*, 2nd ed. (Addison-Wesley, Reading, 1980).
8. D.W. Noid, M.L. Koszykowski, R.A. Marcus, *J. Chem. Phys.* *67*, 404 (1977).
9. C. Hayashi, *Nonlinear Oscillations in Physical Systems*. (Princeton University Press, New Jersey, 1964); A.B. Pippard, *The Physics of Vibration* (Cambridge University Press, Cambridge, 1989)

Figure captions.

Fig.1: A classical trajectory and the position vectors in phase space is projected onto the i -th canonical coordinate plane.

Fig.2: Decomposition of $B(t)$ into the areas represented in the action-angle variables.

Fig.3: The quasi-action variables for various energies. In all the panels, the frequency domain is covered from 0.6 to 1.4. The energy (E) and the height of each panel (H) are: (a) $E=0.1$, $H=0.3$; (b) $E=0.105$, $H=0.3$; (c) $E=0.10583$, $H=0.1$; (d) $E=0.1075$, $H=0.08$; (e) $E=0.125$, $H=0.1$; (f) $E=0.145$, $H=0.08$.

Fig.4: The Poincaré surfaces of section taken at $x=0$ (Panels (a) and (A)), and at $y=0$ (Panels (b) and (B)). For Panels (a) and (b), $E=0.1$, while Panel (A) and (B) have $E=0.105$. The curved line of (a) constitutes almost the inner limit of that of (A), and the manifold of (B) is bounded from the outside by the curve of (b).

A Trajectory in 2N-dimensional Phase Space

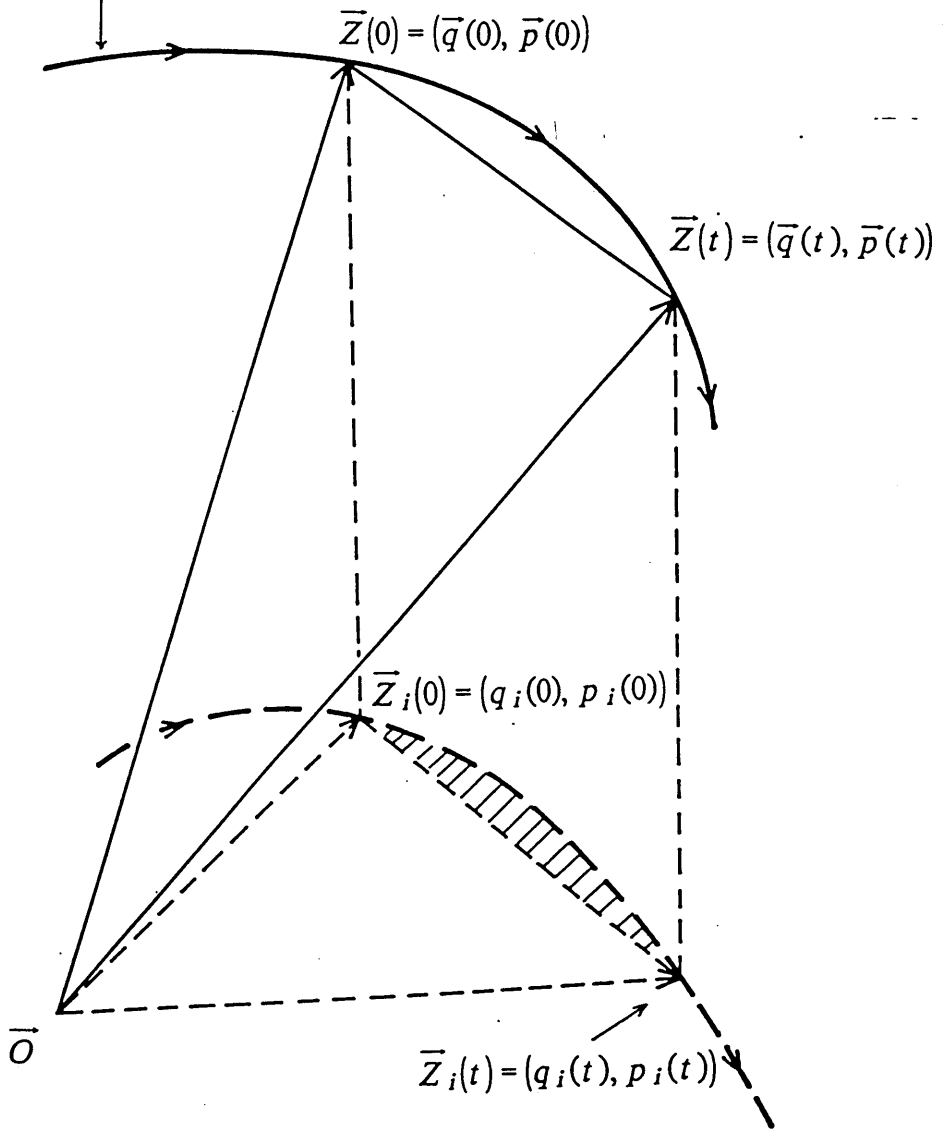


Fig. 1 K. Takatsuka

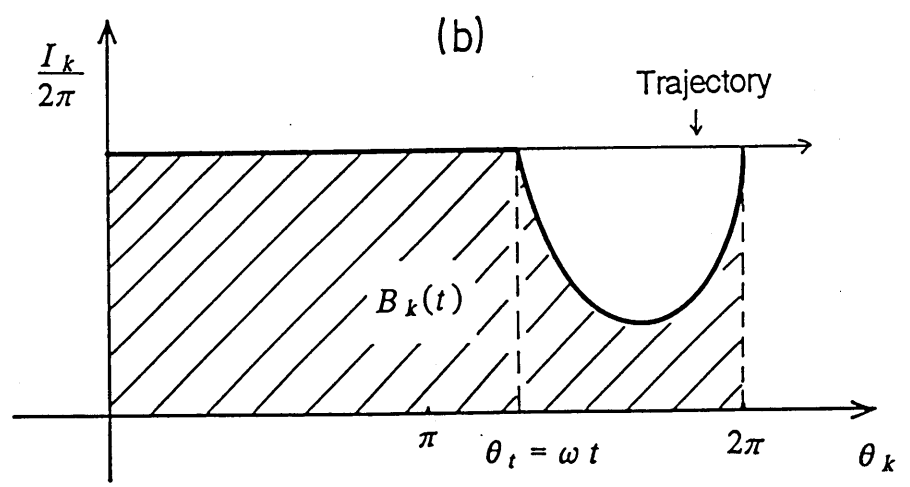
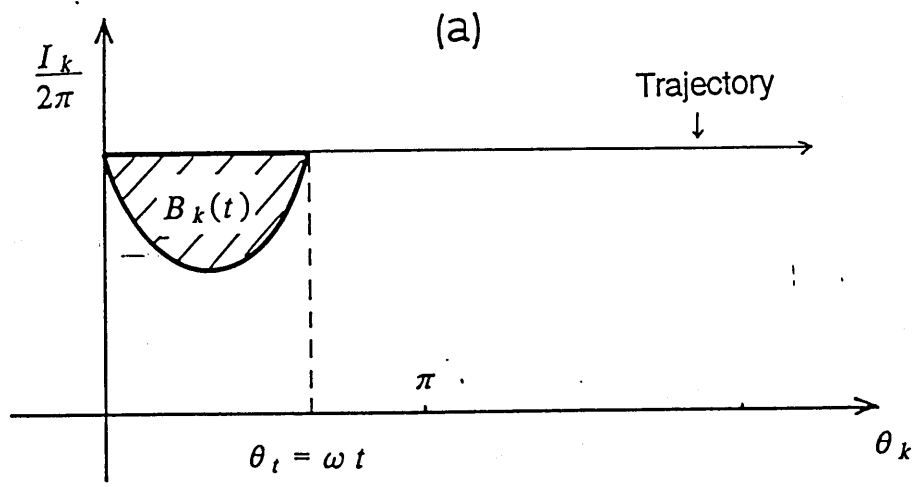
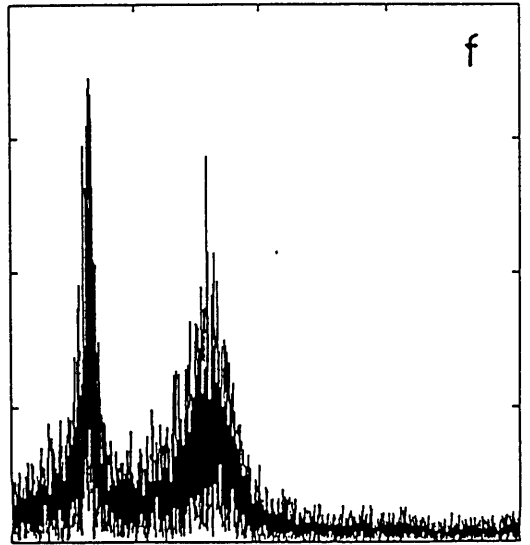
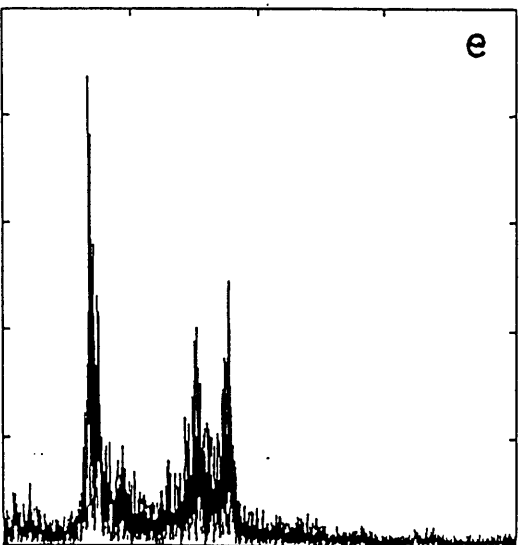
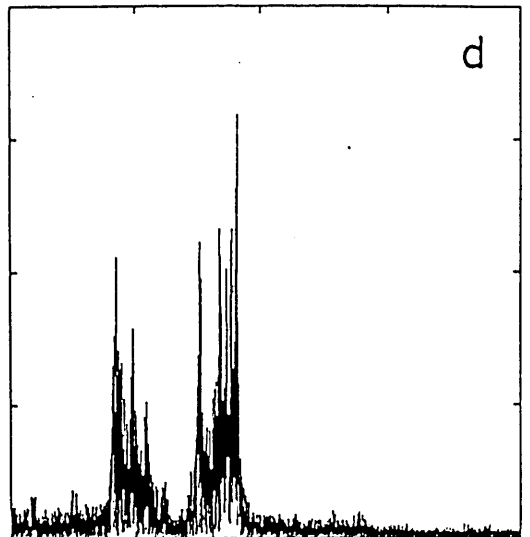
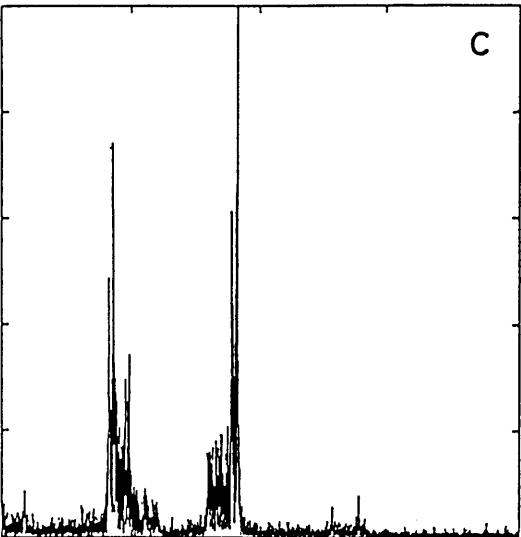
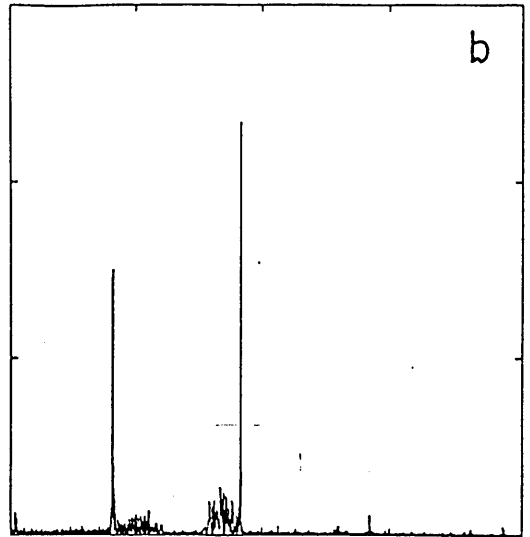
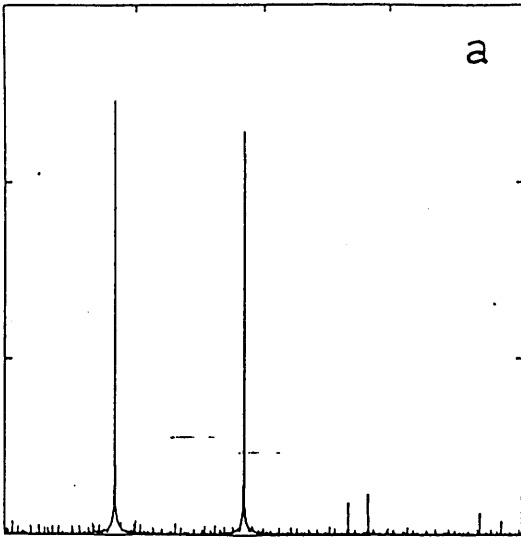


Fig. 2 K. Takatsuka



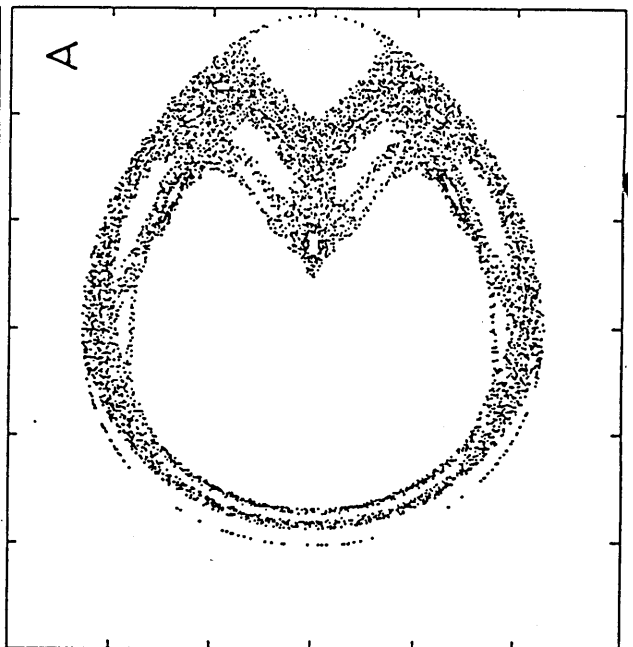
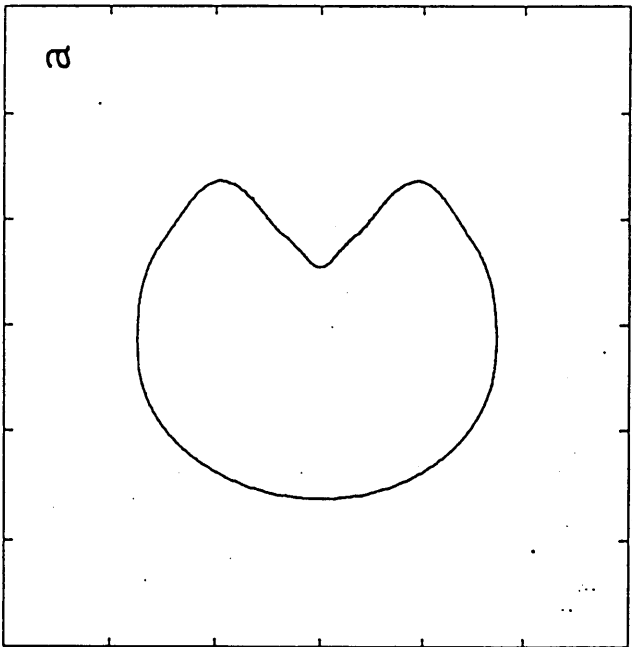
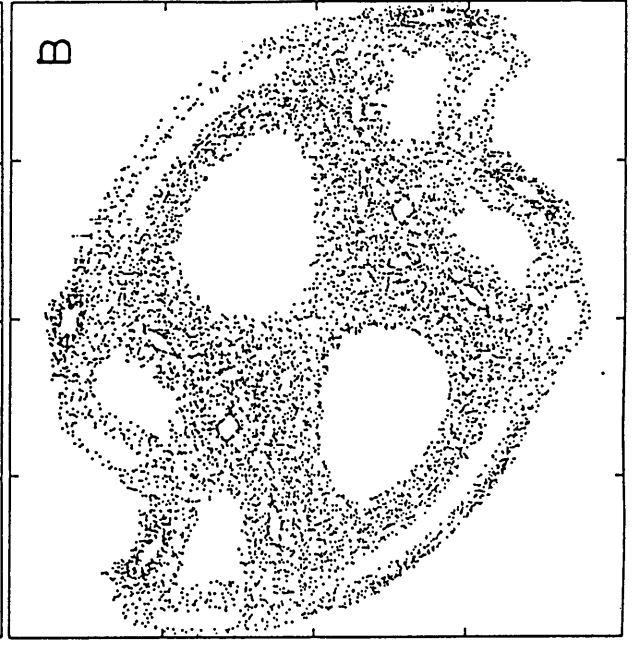
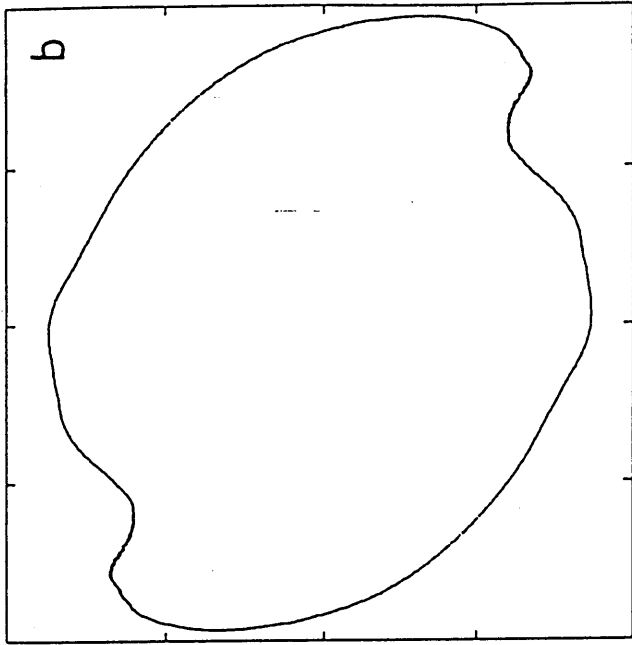


Fig. 4 K. Takatsuki ← up